Designing a parallel manipulator for a specific workspace

Jean-Pierre Merlet

INRIA

INSTITUT NATIONAL DE RECHERCHE EN INFORMATIQUE ET EN AUTOMATIQUE

Designing a parallel manipulator for a specific workspace

Jean-Pierre MERLET

N° 2527

Avril 1995

PROGRAMME 4

ISSN 0249-6399

INRIA
SOPHIA ANTIPOLIS

Designing a parallel manipulator for a specific workspace

Jean-Pierre MERLET

Programme 4 — Robotique, image et vision
Projet Prisme

Rapport de recherche n ° 2527 — Avril 1995 — 61 pages

Abstract: We present an algorithm to determine all the possible geometries of Gough-type 6 D.O.F. parallel manipulators whose workspace has to include a desired workspace. This desired workspace is described by a set of geometric objects, limited here to points, segments and spheres, describing the location of the center of the moving platform, the orientation of the platform being kept constant for each given object. This algorithm takes into account the leg length limits, the mechanical limits on the passive joints and interference between links.

Key-words: workspace, parallel robot

(Résumé : tsvp)

Unité de recherche INRIA Sophia-Antipolis
2004 route des Lucioles, BP 93, 06902 SOPHIA-ANTIPOLIS Cedex (France)
Téléphone : (33) 93 65 77 77 – Télécopie : (33) 93 65 77 65

Conception d'un robot parallèle pour un espace de travail spécifique

Résumé : Nous présentons un algorithme permettant de déterminer toutes les géométries de robots parallèles à 6 degrés de liberté de type plate-forme de Gough dont l'espace de travail doit inclure un espace de travail désiré. Celui-ci est décrit par un ensemble d'objets géométriques, limités ici aux points, segments et sphères, qui représentent la trajectoire d'un point fixe de la plate-forme mobile, l'orientation de celle-ci restant constante sur toute la trajectoire. Cet algorithme prend en compte les limitations sur les longueurs des segments, les débattements limite des articulations passives ainsi que les intersections entre segments.

Mots-clé : espace de travail, robot parallèle

1 Introduction

In this paper we consider a 6 d.o.f. Gough-type parallel manipulator constituted by a fixed base plate and a mobile plate connected by 6 extensible links (figure 1). For a parallel manipulator, workspace limits are due to the bounded range of linear actuators, mechanical limits on passive joints and interference between links. One important step in the design of a parallel manipulator is to define its geometry according to the desired workspace.

Usually the designer will have a choice of linear actuators for the links according to a rough estimate of the articular forces which will occur during the desired task and the desired displacement along the vertical axis. A given choice of linear actuators fully determine the minimum and maximum link lengths. In a second step a set of passive joints will be determined by choosing among commercially available joints. For a given joint mechanical limits are defined. The final step of the process is to determine the location of the attachment points of the links. As soon as these locations are defined the workspace of the robot is fully determined. Usually only a finite set of actuators and joints are available so the main problem of the design process is to determine all the possible location of the attachment points such that the corresponding robots may reach a desired workspace. As soon as this problem is solved some other criterion can be used to find the most suitable robot (such as finding the robot for which the maximum values of the articular forces for a given load is minimal over the workspace).

Note that a similar process is also used for building special-purposes parallel manipulators for which special actuators are designed. According to the desired workspace a rough estimate of the minimum and maximum value of the links lengths are determined and the possible locations of the attachment points are to be determined. We have used this method to determine the geometry of the robot of the European Synchrotron Radiation Facility (ESRF). A numerical procedure was first used to find the locations of the attachment points of the links such that the desired workspace (a cube) can be reached. For this purpose we have used the algorithm described in [11] for computing the workspace, which is an extension of the work of Gosselin [4],[6] enabling to take into account the mechanical limits on the passive joints and interference between links. A grid in the parameters space was defined and each point in the grid was

checked. For each robot whose workspace includes the cube we have computed the maximum positioning error of the platform according to the errors on the articular sensors, this being done for every position in the desired workspace. The main drawbacks of this approach are the computation time and the fact that the grid method does not permit to find all the robots with the correct workspace.

The problem which will be addressed in this paper is to find all the possible locations of the attachment points which fulfill the primary goal (the robot will reach a desired workspace). As soon as this problem has been solved a numerical algorithm can be used to determined which geometry will be "optimal" with respect to other criterion. The main gain of this method is that it will greatly restrict the search domain of the numerical algorithm.

It must be noted that the proposed algorithms have been implemented in C on a workstation under the X-windows system and every drawings appearing in this paper is a result of this program.

This problem has been addressed by very few authors. Claudinon [1] assumes that the attachment points lie on two circle of known radii. The location of one attachment point on its circle is therefore determined by an angle. Claudinon uses a numerical method to find the values of these angles which optimize some kinematics and dynamic features of its robot. Sternheim [14] describes an interactive simulator for computing the workspace of the DELTA 4 robot. Stoughton [15] uses a numerical procedure for optimizing the workspace of a specific parallel manipulator whose length limits are known. Liu [8],[9] characterizes some extremal positions of the platform of a TSSM as a function of the geometry of the robot and the maximum and minimum link lengths. Gosselin [5] studies spherical 3 D.O.F. parallel manipulators which have only rotational degrees of freedom and establishes a design rule to obtain a full rotation of the platform. The same author has studied the optimization of the workspace of planar 3 D.O.F. parallel manipulators [3]. Dubowsky [2] uses a numerical method to find suitable design parameters of a Gough-type platform which has to reach a desired workspace.

We will consider now a Gough-type parallel manipulator (figure 1). Let A_i, B_i denote the attachment points of the link on the base and on the platform. For a set of A_i, B_i we attach a reference frame O, x, y, z to the base such that the z coordinate of A_i is equal to 0. In the same manner we attach to the

platform a mobile frame C, x_r, y_r, z_r such that the z_r coordinate of B_i is equal to 0. A subscript $_r$ will denote a point or a vector whose coordinates are written in the mobile frame. Let α_i be the angle between the Ox axis and OA_i and let β_i be the angle between the Cx_r axis and CB_{i_r}. We denote by R_1, r_1 the distances between (O, A_i), (C, B_i).

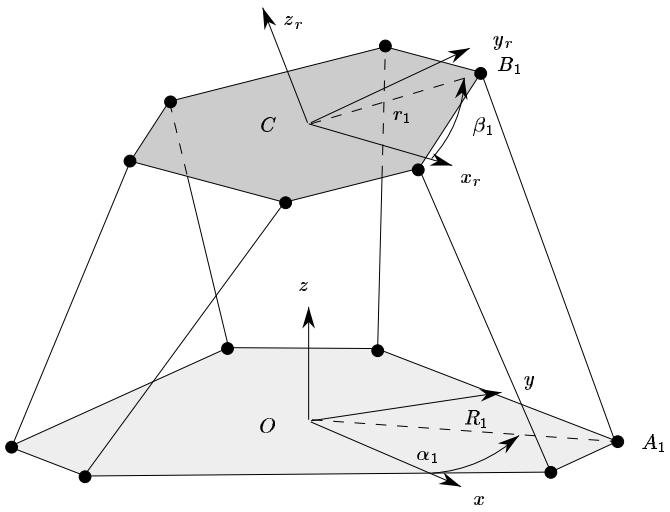

Figure 1: The design parameters for a set of points A_i, Bi are the distances R_1, r_1 between the points and the origins O, C of their frames.

Under these assumptions we have:

$$\mathbf{A_iO} = \begin{pmatrix} -R_1 \cos\alpha_i \\ -R_1 \sin\alpha_i \\ 0 \end{pmatrix} = R_1\mathbf{u_i} \qquad \mathbf{CB_{ir}} = \begin{pmatrix} r_1 \cos\beta_i \\ r_1 \sin\beta_i \\ 0 \end{pmatrix} = r_1\mathbf{v_i} \qquad (1)$$

where $\mathbf{u_i}, \mathbf{v_i}$ are constant unit vectors.

The purpose of this paper is to determine the possible values of R_1, r_1 such that the workspace of the corresponding robot contains a given workspace. The following assumptions are made:

- the minimum and maximum values of the leg lengths are known.

- the angles α_i, β_i are known.

Therefore the design parameters are the distances R_1, r_1. Any point in the R_1, r_1 plane defines a unique location of the attachment points and we have to determine the boundary of the regions of this plane such that their interior define all the robots whose workspace contains the desired workspace. Such region will be called the *allowable region* for the leg.

We will assume that the desired workspace is specified by a set of geometric objects such as points, segments, curves, polygons... describing the location of a fixed point of the platform. In this paper we will restrict ourselves to the case of points, segments and spheres. We will also assume that for each of this object the orientation of the moving platform is kept constant.

2 Points workspace

In the following sections we will assume that the desired workspace W is specified by a set of n points H_i (location of C) with a corresponding orientation matrix R_i of the moving platform:

$$W = \{(H_i, R_i),\ i \in [1, n]\}$$

2.1 Allowable regions for the length constraints

Let us assume that the constraints limiting the workspace are only the leg lengths. The minimum and maximum values of these lengths will be denoted by $\rho_{min_i}, \rho_{max_i}$. The position of the robot is defined by the coordinates of C in the fixed frame and the rotation matrix R between the fixed and mobile frames.

Assume that only one leg has leg length constraints. Let us calculate the leg length when the platform is in a configuration defined by (H, R). The leg length ρ is the norm of the vector $\mathbf{AB}$. We have:

$$\begin{aligned} \rho^2 = ||\mathbf{AB}||^2 \quad = \quad & \mathbf{AO}.\mathbf{AO}^T + \mathbf{HB}.\mathbf{HB}^T + 2(\mathbf{AO} + R\mathbf{HB_r}).\mathbf{OH}^T + \\ & 2R\mathbf{HB_r}.\mathbf{AO}^T + \mathbf{OH}.\mathbf{OH}^T \end{aligned} \tag{2}$$

This equation can be rewritten as:

$$\rho^2 = R_1^2 + r_1^2 + 2R_1r_1\ R\mathbf{v}.\mathbf{u} + 2R_1\mathbf{u}.\mathbf{OH}^T + 2r_1R\mathbf{v}.\mathbf{OH}^T + \mathbf{OH}.\mathbf{OH}^T \quad (3)$$

Let define $\mathcal{E}(H,\rho)$ as:

$$R_1^2 + r_1^2 + 2R_1r_1\ R\mathbf{v}.\mathbf{u} + 2R_1\mathbf{u}.\mathbf{OH}^T + 2r_1R\mathbf{v}.\mathbf{OH}^T + \mathbf{OH}.\mathbf{OH}^T - \rho^2 = 0 \quad (4)$$

For a given ρ this equation defines an ellipse in the R_1, r_1 plane or has none solution in R_1, r_1. It is then easy to prove the following theorem:

Theorem 1 *Let M be a point in the R_1, r_1 plane. If we have $\mathcal{E} \leq 0$ (i.e. M is inside the ellipse), then the length of the leg is less than or equal to ρ for the corresponding posture (H, R).*

Consider now $\mathcal{E}(H_i, \rho_{max})$ which will be called the *maximal ellipse* for (H_i, R_i). For any point M in the R_1, r_1 plane such that $\mathcal{E}(H_i, \rho_{max}) \leq 0$ the leg length is less than of equal to ρ_{max}. Consequently this ellipse defines the allowable region for the maximum length constraint.

Consider now $\mathcal{E}(H_i, \rho_{min})$. This equation defines an ellipse which will be called the *minimal ellipse* for (H_i, R_i). For any point M in the R_1, r_1 plane not belonging to the ellipse (i.e. $\mathcal{E}(H_i, \rho_{min}) > 0$), then the length leg is greater than ρ_{min} for the position H_i. Consequently this ellipse defines the forbidden region for the minimum length constraint.

It is easy now to determine the allowable region in the R_1, r_1 plane. Indeed for each position H_i of the moving platform the points inside the allowable region have to lie inside every maximal ellipses and outside every minimal ellipses. Consequently a valid point belongs to the *intersection* of the maximal ellipses and does not belong to the *union* of the minimal ellipses. In other words the allowable region $\mathcal{A}_l^i$ can be computed as:

$$\mathcal{A}_l^i = \cap_{i=1}^{i=n} \mathcal{E}(H_i, \rho_{max}) - \cup_{i=1}^{i=n} \mathcal{E}(H_i, \rho_{min})$$

Many geometrical techniques can be used to compute $\mathcal{A}_l^i$ without any difficulty. If the attachment points of the base and platform lie on circles we compute the allowable region $\mathcal{A}_l^i$ for each leg. The intersection of these regions will defined the allowable region for all the legs.

2.2 Allowable region for the mechanical limits on the joints

2.2.1 A model for the mechanical limits

We have described in [11] a model for the mechanical limits on the passive joints. They can be described through the definition of a pyramid whose apex is the joint center and whose faces are such that if the joint constraints are satisfied, then the link will be inside the interior of the pyramid. For the joints attached to the base the apex of this pyramid is located at point A_i (Figure 2).

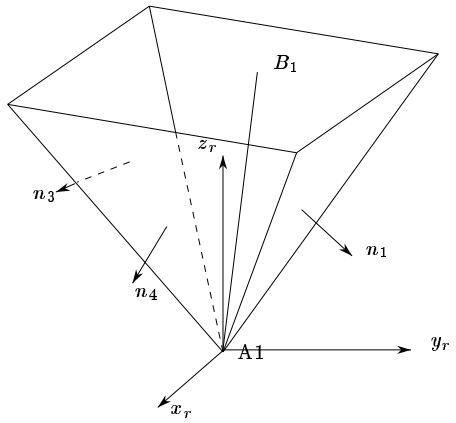

Figure 2: An example of the model for the constraint on a passive joint located at A_1. If the mechanical limits of the joints are satisfied, then link A_1B_1 is inside the volume delimited by the pyramid.

As for the constraints on the passive joints attached to the platform we may use the same model. We define a pyramid P_i with apex B_i such that if the constraint on the joint at B_i are satisfied, then A_i is inside the pyramid. From this pyramid we deduce an *equivalent pyramid* P_i' to P_i, whose apex is A_i, such that if A_i lie inside P_i, then B_i lie inside P_i'.

2.2.2 Allowable region

Consider leg i which is submitted to mechanical limits. Let $\mathbf{n_j^i}, j \in [1,k]$ denote the normals to the faces of the pyramid for the joint i. For a given position of the platform the leg A_iB_i will lie inside the pyramid (which means that the position of the leg respects the mechanical limits of the joints) if:

$$\mathbf{A_iB_i}.\mathbf{n_j^i}^T \leq 0 \quad \forall\ j\ \in\ [1,k]$$

We consider a specific leg and a specific face of a pyramid. The previous inequality can be rewritten as:

$$R_1\mathbf{u}.\mathbf{n}^T + r_1R\mathbf{v}.\mathbf{n}^T + \mathbf{OH_i}.\mathbf{n}^T \leq 0 \tag{5}$$

Let us denote $\mathcal{L}(R_1, r_1, H_i)$ the left side of this inequality. The equation

$$\mathcal{L}(R_1, r_1, H_i) = 0$$

defines a line in the R_1, r_1 plane. This line separates the plane in two half-planes which are such that for one of them $\mathcal{L}(R_1, r_1, H_i) \leq 0$ for any point $M(R_1, r_1)$. Therefore this half-plane is the allowable region for the joint and for this face of the pyramid.

We can now determine the allowable region for one joint: for each face of the pyramid we compute the allowable half-plane, then we compute the intersection of all these half-planes to obtain the allowable region $\mathcal{A}_p^i$ for the joint.

To compute the allowable region for a set of points (H_i, R_i) we use the previous procedure to compute the allowable region $\mathcal{A}_p^i$ for each leg and for each point, then the allowable region $\mathcal{A}_p$ is the intersection of the $\mathcal{A}_p^i$.

2.3 Forbidden region for links interference

2.3.1 Principle of the computation of the forbidden region

In this section we will assume that the links have no thickness. We want to determine the region of the R_1, r_1 plane for which there is no interference between any pair of links, i.e. the zone for which the intersection point M

between the lines i, j, if any, does not belong to both A_iB_i, A_jB_j. We will assume here that the attachment points of the base and platform lie on circles and we consider the case where $i = 1$ and $j = 2$ without loss of generality. The links will interfere if:

- the associated lines interfere
- the common perpendicular points belong to both links

If the two lines intersect then:

$$\mathbf{A_1A_2}.(\mathbf{A_1B_1} \times \mathbf{A_2B_2})^T = 0 \tag{6}$$

which can be written as:

$$-R_1r_1(b_1R_1 + b_2r_1 + b_3) = 0 \tag{7}$$

where the b_i's are constants given by the geometry and the trajectory of the platform. As we may assume that $R_1 \neq 0$ and $r_1 \neq 0$ various cases can be considered. If $b_1 = b_2 = b_3 = 0$ the lines intersect whatever are the dimensions of the robot and if $b_1 = b_2 = 0, b_3 \neq 0$ the lines will never intersect. Otherwise the lines intersect if the R_1, r_1 are on a line in the R_1, r_1 plane.

Now we have to express that the lines intersect at some point belonging to both links. We project the points A_1, A_2, B_1, B_2 onto the plane O, x, y of the reference frame and denote by a superscript ^{P} the projected points. It the segments A_1B_1, A_2B_2 intersect, then their projections will intersect too and the intersection point will belong to the links in three cases. The first one is obtained when:

$$(\mathbf{A_1B_1}^P \times \mathbf{B_1B_2}^P)_z > 0 \qquad (\mathbf{B_2A_2}^P \times \mathbf{B_2B_1}^P)_z < 0 \tag{8}$$
$$(\mathbf{A_1A_2}^P \times \mathbf{A_1B_1}^P)_z < 0 \qquad (\mathbf{A_2A_1}^P \times \mathbf{A_2B_2}^P)_z > 0 \tag{9}$$

where the subscript $_z$ denotes the z component of the vector. The second case is obtained when:

$$(\mathbf{A_1B_1}^P \times \mathbf{B_1B_2}^P)_z < 0 \qquad (\mathbf{B_2A_2}^P \times \mathbf{B_2B_1}^P)_z > 0 \tag{10}$$
$$(\mathbf{A_1A_2}^P \times \mathbf{A_1B_1}^P)_z > 0 \qquad (\mathbf{A_2A_1}^P \times \mathbf{A_2B_2}^P)_z < 0 \tag{11}$$

The last remaining case is obtained when $A_1^P, A_2^P, B_1^P, B_2^P$ are on the same line (in which case the previous inequalities become equalities).

The quantities which appear on the left side of the inequalities can be expressed as functions of R_1, r_1. They have all the same generic form:

$$R_1(e_1R_1 + e_2r_1 + e_3) \quad \text{or} \quad r_1(e_1R_1 + e_2r_1 + e_3)$$

which defines a line. Each inequality will therefore be verified if R_1, r_1 belongs to a half-plane. For each set of inequalities we compute the intersection of the four half-planes with the object described by equation (7). The result defines the forbidden region $\mathcal{F}_i^{12}$ which may be either a region, a line, a segment, a point or the empty set. This process is repeated for each pair of links and for each posture of the desired workspace. The forbidden region for links interference is then the union of all the $\mathcal{F}_i^{jk}$.

3 Segments workspace

In the following sections the desired workspace is described by a set of segments. Note that the validity of the result we will get can be easily checked by using the trajectory verification algorithm described in [12] which enable to verify if a segment is completely inside the workspace of a given robot.

3.1 Allowable regions for the length constraints

3.1.1 Sets of maximal and minimal ellipses

In this section we will assume that the constraints limiting the workspace are only the leg lengths. A trajectory segment is defined by two points $M_1(x_1, y_1, z_1)$, $M2(x_2, y_2, z_2)$ and for any C belonging to the trajectory we may write:

$$\mathbf{OC} = \mathbf{OM_1} + \lambda \mathbf{M_1M_2} \tag{12}$$

where λ is a scalar in the range [0,1]. Let us calculate the leg length for a point C on the segment M_1M_2. The leg length ρ is the norm of the vector $\mathbf{AB}$. We have:

$$\begin{aligned} \rho^2 = ||\mathbf{AB}||^2 \quad = \quad & \mathbf{AO}.\mathbf{AO}^T + \mathbf{CB}.\mathbf{CB}^T + 2(\mathbf{AO} + R\mathbf{CB_r}).\mathbf{OC}^T + \\ & 2R\mathbf{CB_r}.\mathbf{AO}^T + \mathbf{OC}.\mathbf{OC}^T \end{aligned} \tag{13}$$

Using equation (12) this equation can be rewritten as:

$$\begin{aligned}\rho^2 &= R_1^2 + r_1^2 + 2R_1 r_1\ R\mathbf{v}.\mathbf{u} + 2R_1\mathbf{u}.(\mathbf{OM1} + \lambda\mathbf{M_1M_2})^T + \\ &\quad 2r_1 R\mathbf{v}.(\mathbf{OM_1} + \lambda\mathbf{M_1M_2})^T + \lambda^2\mathbf{M_1M_2}.\mathbf{M_1M_2}^T + \\ &\quad \mathbf{OM_1}.\mathbf{OM_1}^T + 2\lambda\mathbf{OM_1}.\mathbf{M_1M_2}^T \end{aligned} \quad (14)$$

This equation can be written in various different forms:

$$R_1^2 + r_1^2 + a_0 R_1 r_1 + R_1(a_1\lambda + a_2) + r_1(a_3\lambda + a_4) + a_5\lambda^2 + a_6\lambda + a_7 = 0 \quad (15)$$

$$\mathcal{E}(R_1, r_1, \lambda, \rho) = 0 \quad (16)$$

$$F(\lambda) = A_2\lambda^2 + A_1\lambda + A_0 = 0 \quad (17)$$

For equation (15) the a_i coefficients are only dependent on the known design parameters and on the coordinates of M_1, M_2. The structure of equation (15) leads to the following theorem:

Theorem 2 *For a given set of ρ, λ the equation defines an ellipse in the R_1, r_1 plane or has no solution in R_1, r_1.*

Proof: We have $a_0 = 2R\mathbf{v}.\mathbf{u}$ and consequently $a_0 \leq 2$ (as $\mathbf{u}$, $\mathbf{v}$ are unit vectors). Any equation of the type:

$$AR_1^2 + Cr_1^2 + 2BR_1 r_1 + DR_1 + Er_1 + F = 0$$

is an ellipse if $B^2 - AC < 0$. Here we have $A = C = 1$, $B \leq 1$ and consequently $B^2 - AC \leq 0$. Therefore equation (15) defines an ellipse. The following theorem is a corollary:

Theorem 3 *Let consider a set of R_1, r_1 (i.e. a point M in the R_1, r_1 plane). If we have $\mathcal{E} \leq 0$ (i.e. the point M is inside the ellipse) for a given λ (i.e. for a fixed position of the platform) then the corresponding length of the leg is lower or equal to ρ.*

Consider now the function $\mathcal{E}_{max}(\lambda) = \mathcal{E}(R_1, r_1, \lambda, \rho_{max})$ in the R_1, r_1 plane with λ in the range [0,1]. This function defines a set of ellipses each of which is called a *maximal ellipse*. If for any λ in the range [0,1] we have $\mathcal{E}_{max}(\lambda) \leq 0$,

then for any position of the platform on the trajectory the leg length is less than or equal to ρ_{max}. Consequently the set of points $M(R_1, r_1)$ such that $\mathcal{E}_{max}(\lambda) \leq 0$ for any λ in [0,1] defines the allowable region for the maximum length constraint. This means that each point M must be inside all the ellipses in the set and therefore the allowable region with respect to the constraint $\rho \leq \rho_{max}$ is the intersection $\mathcal{I}$ of all the ellipses of the set. We denote $\mathcal{E}_{max}(0)$ and $\mathcal{E}_{max}(1)$ the two ellipses obtained for $\lambda = 0$ and $\lambda = 1$.
Let us consider again the set of ellipses defined by:

$$\mathcal{E}(R_1, r_1, \lambda, \rho) = 0 \quad \lambda \in [0, 1]$$

All the ellipses of the set verify the following theorem:

Theorem 4

- *As λ vary the center of the corresponding ellipse lie on a segment which in some cases can be reduced to a point.*
- *The angle between the main axis of the ellipse and the R_1 axis is $\pi/4$.*

Proof: Let us consider the following equation

$$R_1^2 + r_1^2 + a_0\ R_1 r_1 + R_1(a_1\lambda + a_2) + r_1(a_3\lambda + a_4) + a_5\lambda^2 + a_6\lambda + a_7 = 0 \quad (18)$$

where $a_1 = 2\mathbf{u}.\mathbf{OM_1}^T$, $a_3 = 2R\mathbf{v}.\mathbf{OM_1}^T$ and $a_0 \leq 2$. To determine the center of the ellipse for a particular λ we first search the translation which eliminate the first order term of the equation. Let x_a, y_a be the coordinate of the center of the ellipse and let define $R_1 = x + x_a, r_1 = y + y_a$. Using this substitution equation (18) becomes an equation in the unknowns x, y:

$$x^2 + y^2 + b_1\ xy + b_2 x + b_3 y + b_4 = 0 \quad (19)$$

with

$$\begin{aligned} b_2 &= 2\,x_a + a_0\,y_a + a_1\,\lambda + a_2 \\ b_3 &= 2\,y_a + a_0\,x_a + a_3\,\lambda + a_4 \end{aligned}$$

We want to determine x_a, y_a such that these coefficients are equal to 0. This system is linear in x_a, y_a and has a determinant equal to $4 - a_0^2$ which is always greater than 0. The solution of this system is:

$$\begin{aligned} x_a &= \frac{-a_0 a_3 \lambda + 2 a_1 \lambda + 2 a_2 - a_0 a_4}{-4 + a_0^2} \\ y_a &= -\frac{a_0 a_1 \lambda + a_0 a_2 - 2 a_3 \lambda - 2 a_4}{-4 + a_0^2} \end{aligned}$$

If $a_0 a_3 - 2a_1 \neq 0$ x_a, y_a lie on a line defined by:

$$y_a = -\frac{x_a(2a_3 - a_0 a_1) + a_3 a_2 - a_1 a_4}{a_0 a_3 - 2a_1}$$

if $a_0 a_3 - 2a_1 = 0$ the line is defined by:

$$x_a = \frac{2a_2 - a_0 a_4}{a_0^2 - 4}$$

If $a_0 a_3 - 2a_1 = 0$ and $a_0 a_1 - 2a_3 = 0$ (which leads to $a_1 = a_3 = 0$) the center of the ellipse is the same for every value of λ. This complete the proof of the first part of the theorem.

After substitution of x_a, y_a equation (19) becomes:

$$b_1 x^2 + b_2 y^2 + b_3 xy + b_4 = 0 \tag{20}$$

Now a rotation is performed on the frame. We define:

$$\begin{aligned} x &= X \cos\gamma - Y \sin\gamma \\ y &= X \sin\gamma + Y \cos\gamma \end{aligned}$$

After substitution equation (20) becomes:

$$c_1 X^2 + c_2 Y^2 + c_3 XY + c_4 = 0$$

with

$$c_3 = a_0 \left(2\cos^2(\gamma) - 1\right) (a_0 - 2)^2 (a_0 + 2)^2$$

If $2\cos^2\gamma - 1 = 0$ then $c_3 = 0$. Consequently the orientation of the ellipse is equal to $\pi/4$, which conclude the proof of the theorem.

Now we have to determine under which condition the intersection of the maximal ellipses exists and how to compute this intersection. We will first show the following theorem:

Theorem 5 *If the ellipse exists for $\lambda = 0$ and $\lambda = 1$ then the ellipse exists for any value of λ in the range [0,1] or the intersection of all the ellipses of the set is empty.*

Proof: The existence of the ellipse for $\lambda = 0$ and $\lambda = 1$ means that there exist two sets S_1, S_2 of (R_1, r_1) such that:

$$\begin{aligned} \forall\ u = (R_1, r_1) \ &\in\ S_1 \quad F(0) \leq 0 \\ \forall\ u = (R_1, r_1) \ &\in\ S_2 \quad F(1) \leq 0 \end{aligned}$$

Assume that $S_3 = S_1 \cap S_2 = \emptyset$ then the intersection of $\mathcal{E}_{max}(0), \mathcal{E}_{max}(1)$ is empty and consequently the intersection of all the ellipses of the set is empty. We may now assume that S_3 is not empty. Consequently:

$$\begin{aligned} \forall\ u = (R_1, r_1) \ &\in\ S_3 \quad F(0) \leq 0 \\ \forall\ u = (R_1, r_1) \ &\in\ S_3 \quad F(1) \leq 0 \end{aligned}$$

For a particular $u = (R_1, r_1) \in S_3$ let denote λ_1, λ_2 the two real roots of $F(\lambda)$. As the coefficient of λ^2 of $F(\lambda)$ is strictly positive we have:

$$F(\lambda) \leq 0 \quad \forall\ \lambda\ \in\ [\lambda_1, \lambda_2]$$

As $F(0) \leq 0$ and $F(1) \leq 1$ we conclude that [0,1] $\subset [\lambda_1, \lambda_2]$. Therefore for any λ in [0,1] and any $u \in S_3$, $F(\lambda) \leq 0$. Assume now that it exists a λ in the range [0,1] such that the ellipse $F(\lambda)$ does not exist. This imply that there is no (R_1, r_1) such that $\mathcal{E}(R_1, r_1, \lambda, \rho_{max}) \leq 0$. As the coefficient of R_1^2, r_1^2 of $\mathcal{E}$ are strictly positive we deduce that for any $u = (R_1, r_1)$ we have $\mathcal{E}(R_1, r_1, \lambda, \rho_{max}) > 0$. But we have previously demonstrated that for any $u \in S_3$ $\mathcal{E}(R_1, r_1, \lambda, \rho_{max}) \leq 0$. Consequently the ellipse will always exist for any $\lambda \in [0, 1]$.

Now the problem is computing the intersection of all the ellipses of the set under the assumption that the ellipses exist for $\lambda = 0$ and $\lambda = 1$. Consider the two particular ellipses $\mathcal{E}_{max}(0)$ and $\mathcal{E}_{max}(1)$ and let $\mathcal{I}$ be the intersection of all the ellipses in the set. We will prove the following theorem:

Theorem 6 *The intersection $\mathcal{I}$ of all the ellipses in the set is equal to*

$$\mathcal{E}_{max}(0) \cap \mathcal{E}_{max}(1)$$

Proof: Let $\mathcal{I}_{01} = \mathcal{E}_{max}(0) \cap \mathcal{E}_{max}(1)$. Clearly we have

$$\mathcal{I} \subset \mathcal{I}_{01}$$

Consider a point M inside $\mathcal{I}_{01}$. For this particular point $\mathcal{E}_{max}(\lambda)$ is a second order polynomial in λ which is denoted $F(\lambda)$ and we have $F(0) \leq 0$ and $F(1) \leq 0$. Let us denote λ_1, λ_2 the two real roots of F. As the leading coefficient of $F(\lambda)$ is strictly positive F will be lower of equal to 0 for any λ in the range $[\lambda_1, \lambda_2]$. As $F(0) \leq 0, F(1) \leq 0$ the interval [0,1] is included in $[\lambda_1, \lambda_2]$ and consequently for any λ in [0,1] F is lower or equal to 0. This means that for any M in $\mathcal{I}_{01}$, $\mathcal{E}_{max}(\lambda) \leq 0$ for any λ in [0,1]. In other terms M belongs to all the ellipses in the set. Therefore:

$$\mathcal{I}_{01} \subset \mathcal{I}$$

which conclude the proof.

Therefore the allowable region is simply the intersection of the ellipses computed for the extreme points of the trajectory. Note that due to the particular structure of the equation of the ellipse there will be at most two intersection points between two maximal ellipses. The following interesting theorem hold (the proof is given in the annex).

Theorem 7 *If a trajectory is such that the base and the platform are parallel and $z_1 = z_2$ then the dimensions of every ellipses in the set $\mathcal{E}(R_1, r_1, \lambda, \rho)$ are constant all along the trajectory. These dimensions will be constant whatever is the trajectory.*

Consider now the function $\mathcal{E}_{min}(\lambda) = \mathcal{E}(R_1, r_1, \lambda, \rho_{min})$ in the R_1, r_1 plane. This function defines a set of ellipses, each of which is called a *minimal ellipse*. If for a given point M and a given λ we have $\mathcal{E}_{min}(\lambda) > 0$, then the corresponding length leg is greater than ρ_{min}. Therefore for any point belonging to the allowable region this relation as to be verified for all λ in [0,1]. Consequently any point in the allowable region must lie outside the region $\mathcal{U}$ defined by the

union of the minimal ellipses. The final allowable region $\mathcal{A}_l$ is therefore defined by:

$$\mathcal{A}_l = (\mathcal{E}_{max}(0) \cap \mathcal{E}_{max}(1)) - \mathcal{U} \tag{21}$$

Note that the minimal ellipse may not exist for any λ. Indeed let us write $\mathcal{E}_{min}(\lambda)$ as:

$$R_1^2 + r_1^2 + C_1 R_1 r_1 + D_1 R_1 + E_1 r_1 + F_1 = 0 \tag{22}$$

where $C_1 \leq 2$ is not dependent of λ and:

$$\begin{aligned} D_1 &= d_1\lambda + d_0 \\ E_1 &= e_1\lambda + e_0 \\ F_1 &= f_2\lambda^2 + f_1\lambda + f_0 - \rho_{min}^2 \end{aligned}$$

Equation (22) may be considered as a second order equation in R_1. Its discriminant Δ is:

$$\Delta = (C_1 r_1 + D_1)^2 - 4(r_1^2 + E_1 r_1 + F_1)$$

which should be positive if the ellipse exists. It can be seen that Δ is a second order equation in r_1, whose leading term coefficient is strictly negative. Therefore if the real roots of Δ are denoted r_1^1, r_1^2 then Δ is positive for r_1 in $[r_1^1, r_1^2]$. Consequently the minimal ellipse will exist only if the discriminant Δ_1 of Δ is positive. Δ_1 is a second order polynomial in λ whose leading term coefficient is strictly negative. If λ_1, λ_2 are the real roots of Δ_1 then Δ_1 is positive for any λ in $[\lambda_1, \lambda_2]$. If no such root exist then there is no minimal ellipse. If the roots exist then the intersection of $[\lambda_1, \lambda_2]$ with the interval [0,1] define the range $[\lambda_m, \lambda_M]$ for λ for which the minimal ellipse exists. Note that the intersection will define only one interval for λ.

3.1.2 The "growing" algorithm

Obtaining the region $\mathcal{U}$ is the main difficulty of the computation of $\mathcal{A}_l$. For this purpose we will now describe an efficient method, the "growing" algorithm which was first suggested by Troyanov [16]. The constraint which defines the region $\mathcal{U}$ is $||\mathbf{AB}||^2 \leq \rho_{min}^2$. The vector $\mathbf{AB}$ can be written as:

$$\mathbf{AB} = R_1\mathbf{u} + \mathbf{OC} + r_1\mathbf{v} \tag{23}$$

Let Π be the plane defined by the origin O and the vectors $\mathbf{u}, \mathbf{v}$. Let M be a point of this plane such that $\mathbf{MO} = R_1\mathbf{u} + r_1\mathbf{v}$. The forbidden region may now be defined as the set of points M (which defines a unique value of R_1, r_1) such that

$$||\mathbf{AB}||^2 = ||\mathbf{MC}||^2 \leq \rho_{min}^2 \tag{24}$$

Clearly for a fixed C the set of points M is the intersection of the plane Π with the sphere of radius ρ_{min} centered at C. When C lie on a segment M_1M_2 the set of point M is obtained by "growing" the segment by ρ_{min} i.e. by first constructing the 3D volume, called the "grown" volume, of the points which are at a distance less than or equal to ρ_{min}, then by intersecting this volume with the plane Π. The "growing" of a segment leads to a portion of cylinder of height $||\mathbf{M_1M_2}||$ and radius ρ_{min} topped by two half spheres of radius ρ_{min} centered at M_1, M_2 (figure 3).

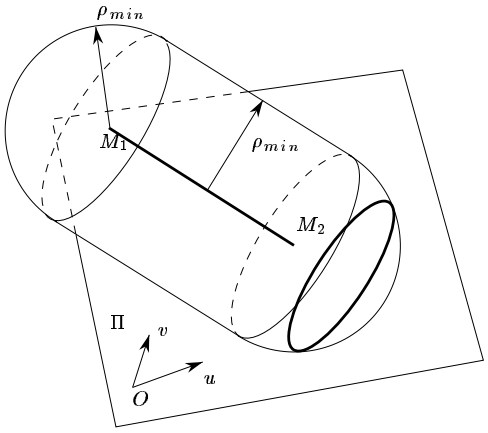

Figure 3: The growing of a segment M_1M_2 by ρ_{min} leads to a volume composed of a portion of cylinder topped by two half spheres. The intersection of this volume with the plane Π gives a region (here the ellipse in thick lines). The boundary of this region computed in the $O, \mathbf{u}, \mathbf{v}$ frame is the forbidden region.

Practically we first define a vector $\mathbf{w}$ as $(\mathbf{u} \times \mathbf{v})/||\mathbf{u} \times \mathbf{v}||$ and use the Cartesian frame $O, \mathbf{u}, \mathbf{w} \times \mathbf{u}, \mathbf{w}$. The intersection of the grown volume and the Π plane is computed in this frame and is approximated by a polygon. The

coordinates of the vertices of this polygon are then expressed in the frame $O, \mathbf{u}, \mathbf{v}$ which leads to a polygon in the R_1, r_1 plane. This polygon defines the forbidden region.

3.1.3 Examples

Figures 4,5,6 show examples of this algorithm for various types of robot and trajectories.

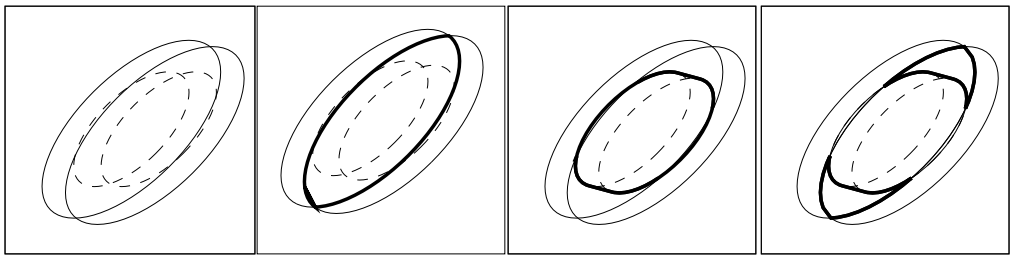

Figure 4: The computation of the allowable region. On the left side are drawn the maximal ellipses for the extreme point of the trajectory (in thin line) and the minimal ellipses for the same points (in dashed line). The intersection of the maximal ellipses is shown on the second drawing. The union of the forbidden ellipses is shown on the third drawing. The final allowable region is shown in thick line on the last drawing (first segment, trajectory 0, first set of length limits).

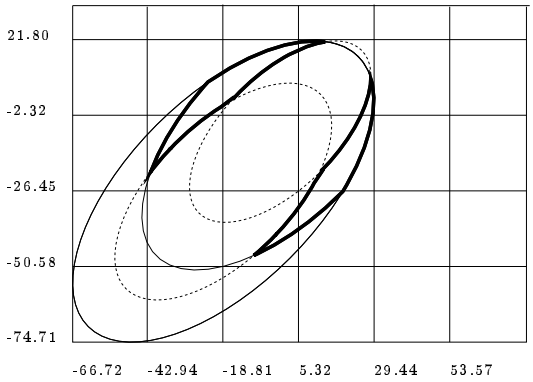

Figure 5: The maximal ellipse is shown in thin line, the minimal ellipse in dashed line and the allowable region in thick line (trajectory 2, first set of length limits, first segment).

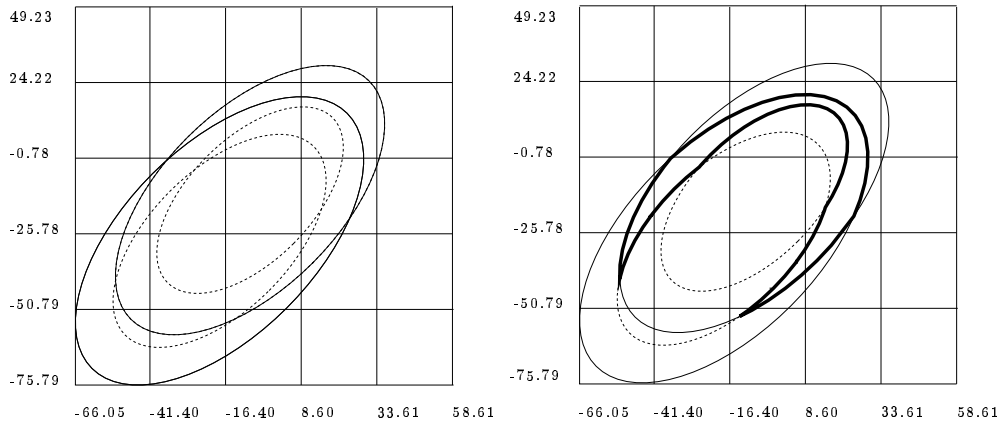

Figure 6: The maximal ellipse is shown in thin line, the minimal ellipse in dashed line and the allowable region in thick line (trajectory 5, first set of length limits, first segment).

3.1.4 Computation of the allowable region for a set of segments

The computation of the allowable region for the leg length constraints is done using the following algorithm:

1. for each trajectory compute the allowable region using the following algorithm
   (a) compute the maximal ellipses for the extreme points of the trajectory
   (b) compute the intersection $\mathcal{I}$ of these two ellipses. If there is none there is no allowable region.
   (c) compute the union $\mathcal{U}$ of the minimal ellipses using the "growing" algorithm
   (d) subtract $\mathcal{U}$ to $\mathcal{I}$ to get the allowable region
2. compute the intersection of all the allowable regions

In our implementation all the regions are approximated by polygons in order to simplify the intersection and the boolean operations on the regions.

Figure 7 shows an example of allowable region when two trajectories has been specified. Figure 8 shows that for a robot defined by a point in the allowable region the two trajectories are indeed in the workspace. In the example presented in figure 9 three segments have been defined.

Another example is shown on figure 10. We have defined 64 trajectories with identical start point (0,0,50) and end points uniformly distributed on the sphere with radius 5 centered at the start point. On this figure we show the 3D representation of the workspace of a particular robot defined by a point in the allowable region together with the 64 trajectories (in thick lines).

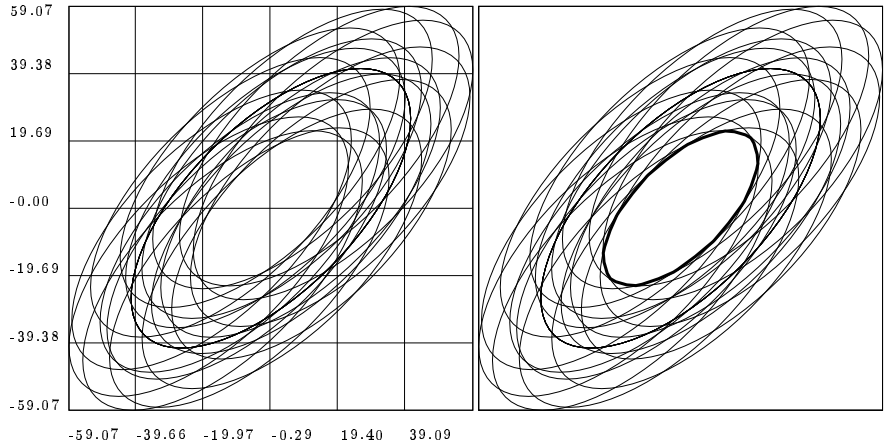

Figure 7: In this example there is no minimal ellipse and two trajectories have been specified. On the left the maximal ellipses for the extreme points of the trajectories are shown and the allowable region is drawn in thick line (trajectory 8, second set of length limits).

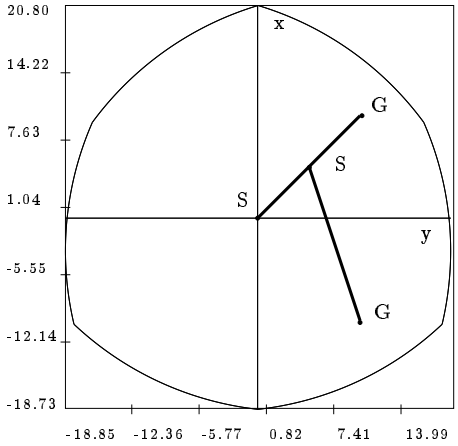

Figure 8: For a given robot defined by a point in the allowable region the two trajectories (in thick lines) are effectively inside the workspace boundary.

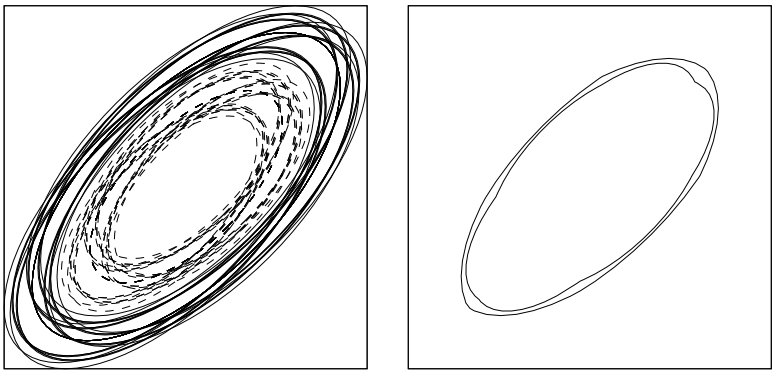

Figure 9: On the left the minimal ellipses (dashed lines) and the maximal ellipses (in thin lines) for a workspace defined by three segments. On the right the allowable region.

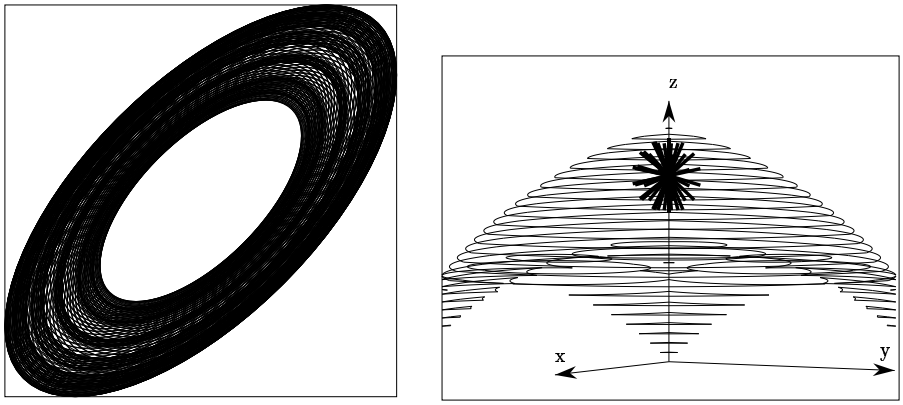

Figure 10: 64 trajectories with identical start point and end point uniformly distributed on a sphere centered at the start point with radius 5 have been defined. The central area defines the robots which include all the 64 trajectories. For a given robot defined by a point in the allowable region the 64 trajectories (in thick lines) approximating a sphere are effectively inside the workspace boundary.

3.2 Allowable region for the mechanical limits on the joints

In this section we will use the model for the mechanical limits described in the points workspace. For a given position of the platform the leg A_iB_i will lie inside the pyramid (which means that the position of the leg fulfill the mechanical limits of the joints) if:

$$\mathbf{A_iB_i}.\mathbf{n_j^i}^T \leq 0 \quad \forall\, j \in [1,k]$$

We consider a specific leg and a specific face of a pyramid. Using equation (12) the previous inequality can be rewritten as:

$$R_1\mathbf{u}.\mathbf{n}^T + r_1R\mathbf{v}.\mathbf{n}^T + \lambda\mathbf{M_1M_2}.\mathbf{n}^T + \mathbf{OM_1}.\mathbf{n}^T \leq 0 \tag{25}$$

Let us denote $\mathcal{L}(R_1, r_1, \lambda)$ the left side of this inequality. The equation $\mathcal{L}(R_1, r_1, \lambda) = 0$ defines a pencil of lines in the R_1, r_1 plane. All these lines have a constant slope. This pencil of lines defines a region in the plane whose boundary is constituted of the line $\mathcal{L}(R_1, r_1, 0) = L_0$, $\mathcal{L}(R_1, r_1, 1) = L_1$. If $\mathbf{M_1M_2}.\mathbf{n}$ is positive (negative), then L_1 (L_0) will define two half planes one of which is the allowable region for this face of the pyramid (figure 11).

The process is repeated for each faces of the pyramid, leading to a set of half-planes. The intersection of these half-planes will be a closed region which define the allowable region with respect to the mechanical limits on the joints. An example of this computation is shown in figure 12.

As a specific case we may assume that all the joints lie on two horizontal circles and we want to determine the possible radii of these two circles. The process is to compute all the set of allowable half-planes for all the joints and all the trajectories and compute their intersection. An example is shown in figure 13. Evidently we can combine the results of the two previous sections. We first compute the allowable region for the leg lengths constraints, then the allowable region for the mechanical limits constraints. The intersection of the allowable regions defines the allowable region for all the constraints. An example of such computation is shown on figure 14. The validity of the result is shown on figure 15. Another example is presented in figure 16 for 25 trajectories defining a sphere centered at (12,12,50), with radius 5. These

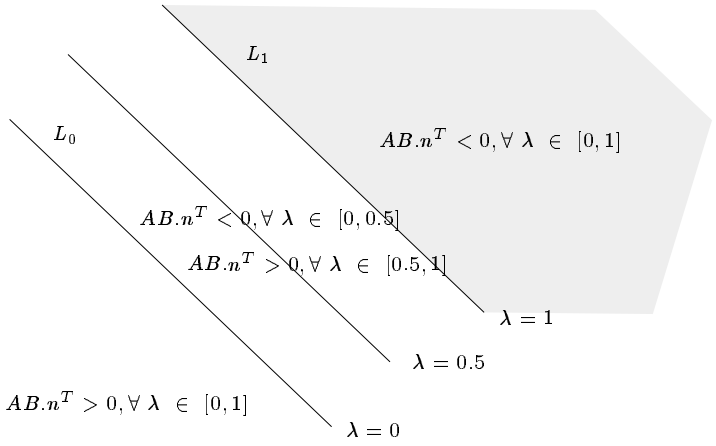

Figure 11: The lines L_0, L_1 define in the plane R_1, r_1 a region in the plane. One of these lines (here L_1) defines an half-plane (in gray) such that any point M in this half-plane respects the constraint for a face of the pyramid.

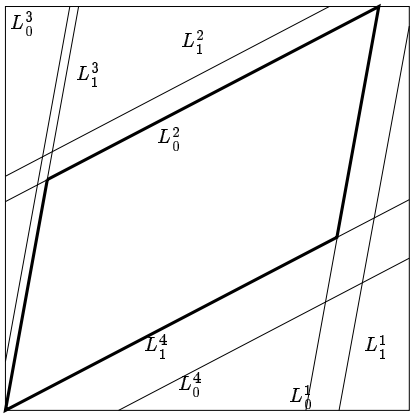

Figure 12: The mechanical limits of a particular joint is described by a four-faced pyramid. We have computed the separating half-plane for each of the faces by computing the L_0, L_1. The intersection of these half-planes define a closed region (in thick line) which is the allowable region for this joint.

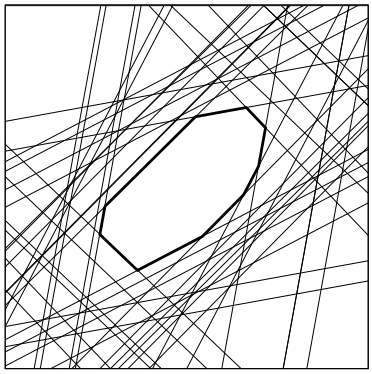

Figure 13: The attachment points are on the same circle. In the R_1, r_1 plane the computation of the intersection of the separating half-plane leads to a region (in thick line) which define all the possible dimensions of the robots for which the links will respect the mechanical limits of all the joints on the specified trajectories.

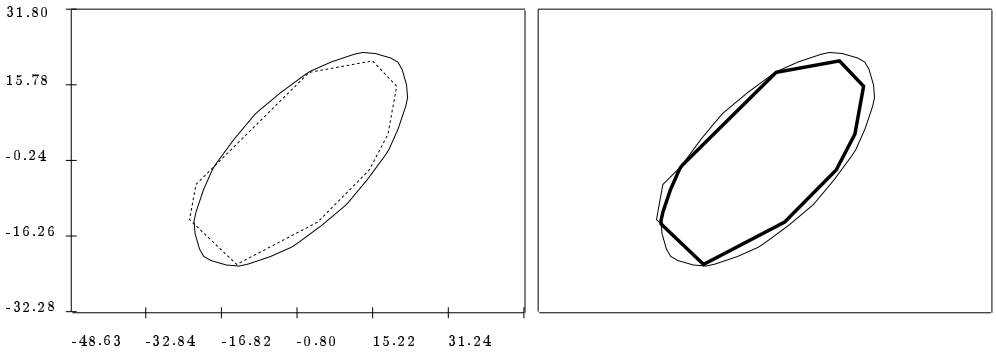

Figure 14: An example of computation of allowable region combining the leg lengths constraints and the mechanical limits. On the left the allowable region for the leg lengths constraints and mechanical limits constraints (in dashed lines) are shown. On the right the allowable region for all these constraints is shown in thick lines (trajectory 8, second set of length limits).

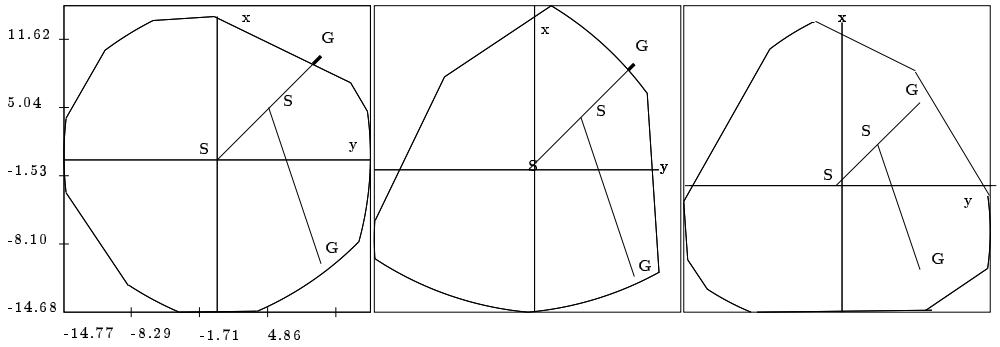

Figure 15: Example of robots chosen according to the result. On the left a robot satisfying the leg lengths constraints but not the mechanical limits has been selected: one of the trajectory is outside the workspace. In the middle the robot satisfy the mechanical limits but not the leg lengths constraints. At the right a robot defined by a point in the allowable region has be chose: the trajectories are all inside the workspace.

figures shows the allowable region for the length constraints and the allowable region for the mechanical limits constraints (in thin lines) together with the allowable region for both constraints (in thick lines). We have chosen two points A_1, A_2 defined by $(R_1 = 1.82, r_1 = 1.82)$ which lie inside the allowable region for both constraints and $(R_1 = 4.47, r_1 = 4.71)$ which lie inside the allowable region for the length constraints but not in the allowable region for the mechanical limits. Figure 17 shows that these points really define robots which respect the constraints defined by the region to which they belong.

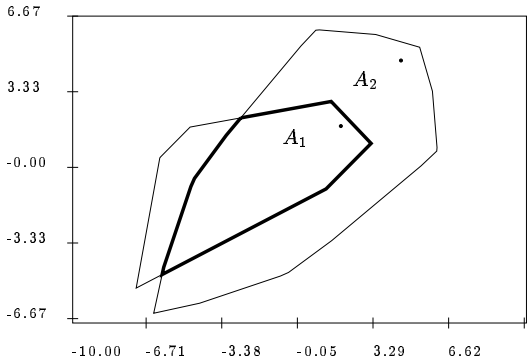

Figure 16: In thin lines the allowable region for the length constraints and the allowable region for the mechanical limits constraints and in thick lines the allowable region for both constraints.

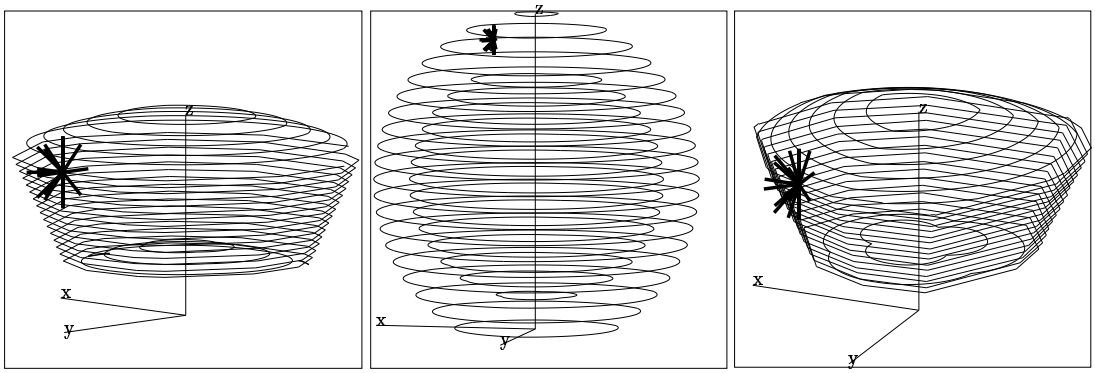

Figure 17: On the left the 3D workspace for the robot defined by point A_1: the specified workspace lie well within the robot workspace. In the middle the 3D workspace for the robot defined by A_2 when only the length constraints are taken into account: the specified workspace lie inside the robot's workspace. On the right side the 3D workspace for all the constraints: the specified workspace lie outside the robot's workspace.

3.3 Forbidden region for interference between links

We will consider the case where $i = 1$ and $j = 2$ without loss of generality. If the two lines intersect then:

$$\mathbf{A_1A_2}.(\mathbf{A_1B_1} \times \mathbf{A_2B_2})^T = 0 \tag{26}$$

which can be written as:

$$-R_1r_1(b_1\lambda + b_2R_1 + b_3r_1 + b_4) = 0 \tag{27}$$

where the b_i's are constants given by the geometry and the trajectory of the platform. Various cases can now be considered:

1. $b_1 = b_2 = b_3 = b_4 = 0$: the lines intersect whatever is the dimension of the robot for any position on the trajectory of the robot.
2. $b_1 = 0$: the lines will intersect if the R_1, r_1 are on a line in the R_1, r_1 plane
3. in the general case the lines will intersect if the R_1, r_1 are on a pencil of lines in the R_1, r_1 plane

Each of these cases defines a region $\mathcal{R}$ in the R_1, r_1 plane for which the two lines intersect. In the first case this region is the full plane, in the second case the region is the line $b_2R_1 + b_3r_1 + b_4 = 0$ and in the last case the region is the zone delimited by the line $b_1 + b_2R_1 + b_3r_1 + b_4 = 0$ and $b_2R_1 + b_3r_1 + b_4 = 0$ which are the extremal lines of the pencil. Consequently computing this region is easy. But we are interested only in the sub region where the links intersect. To determine this region we use the inequalities (8,9), (10,11).

The quantities which appear on the left side of the inequalities can be expressed as function of λ, R_1, r_1. They have all the same generic form:

$$R_1(e_1\lambda + e_2R_1 + e_3r_1 + e_4) \quad \text{or} \quad r_1(e_1\lambda + e_2R_1 + e_3r_1 + e_4)$$

which defines a pencil of lines. It must be first noted that the inequalities may define unbounded region. As the other constraints on the workspace lead to bounded region we will consider only a limited portion of the R_1, r_1 plane, for

example a square whose dimensions is equal to the maximum dimension of the rectangle which enclosed all the maximal ellipses. After the computation of $\mathcal{R}$ we consider each set of inequalities. We divide then the square in four regions Q_i defined by:

$$\begin{array}{ll} R_1 \geq 0 \;\; r_1 \geq 0 & \qquad R_1 \geq 0 \;\; r_1 \leq 0 \\ R_1 \leq 0 \;\; r_1 \geq 0 & \qquad R_1 \leq 0 \;\; r_1 \leq 0 \end{array}$$

In each region Q_i the sign of the inequalities is now fully defined by four inequalities:

$$e_1^i \lambda + e_2^i R_1 + e_3^i r_1 + e_4^i \leq \; 0$$

By dealing with this four inequalities we are able to determine four half-planes in which each inequality is satisfied. Then we compute the intersection of these half-planes together with the region defined by equation (27). The result is the forbidden region of the plane. Note that a reasonable assumption will lead to restrict the study to the region Q_i where $R_1 > 0, r_1 > 0$. We will distinguish now various cases according to the region defined by equation (27).

3.3.1 Pencil case

In this case $\mathcal{R}$ is bounded by the two lines with same slope $b_2 R_1 + b_3 r_1 + b_4 = 0$ and $b_2 R_1 + b_3 r_1 + b_4 + b_1 = 0$. If the lines intersect for some value λ_1 of λ then we have:

$$b_1 \lambda_1 + b_2 R_1 + b_3 r_1 + b_4 = 0$$

From this equation we deduce the value of λ_1 as function of R_1, r_1 which is reported in the inequalities. These inequalities now define four half planes in the R_1, r_1 plane. The intersection of these half-planes with $\mathcal{R}$ define the region where links interference will occur. Figure 18 shows an example of such case.

3.3.2 Full plane case

For each of the inequality one of the line obtained either for $\lambda = 0$ or $\lambda = 1$ defines a half plane in the R_1, r_1 plane such that for any point in the half plane the inequality will be satisfied. In each of this region Q_i the sign of the inequality is now fully defined by four generic inequalities:

$$e_1^i \lambda + e_2^i R_1 + e_3^i r_1 + e_4^i \geq 0 \qquad (28)$$

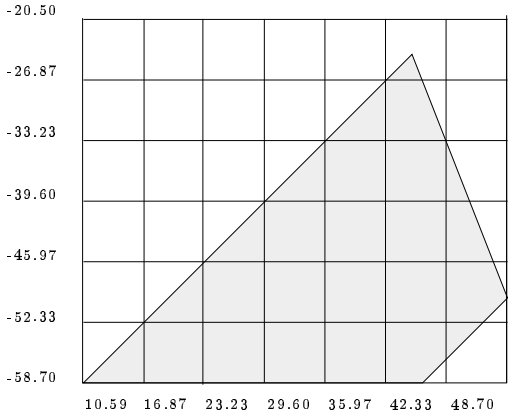

Figure 18: Example of links interference zone. $\mathcal{R}$ is defined by a pencil of lines (bounded here by the the two lines with a positive slope). The intersection of $\mathcal{R}$ with the half-planes defined by the inequalities defines the gray region where interference will occur (link 0 and 4, trajectory 2).

If $e_1^i > 0$ then we must have:

$$\lambda > \frac{-e_2^i R_1 - e_3^i r_1 - e_4^i}{e_1^i}$$

As λ should lower or equal to 1 we get:

$$-e_2^i R_1 - e_3^i r_1 - e_4^i < e_1^i$$

the region for which this inequality is satisfied is the half-plane whose boundary is the line

$$-e_2^i R_1 - e_3^i r_1 - e_4^i - e_1^i = 0$$

If $e_1^i < 0$ then we must have:

$$\lambda < \frac{e_2^i R_1 + e_3^i r_1 + e_4^i}{-e_1^i}$$

As λ should greater or equal to 0 we get:

$$\frac{e_2^i R_1 + e_3^i r_1 + e_4^i}{-e_1^i} > 0$$

the region for which this inequality is satisfied is an half-plane. If $e_1^i = 0$ the region for which equation (28) is verified is also an half-plane.

The intersection of the set of half-planes with Q_i defines the region for which the inequalities (8, 9),(10, 11) are satisfied. This process is repeated for the four regions Q_i. By repeating this process for every pair of links and taking the union of the results we get the region of the R_1, r_1 plane for which at least one pair of links will interfere.

Figures 19,20 show examples of such computation. Figure 21 shows that

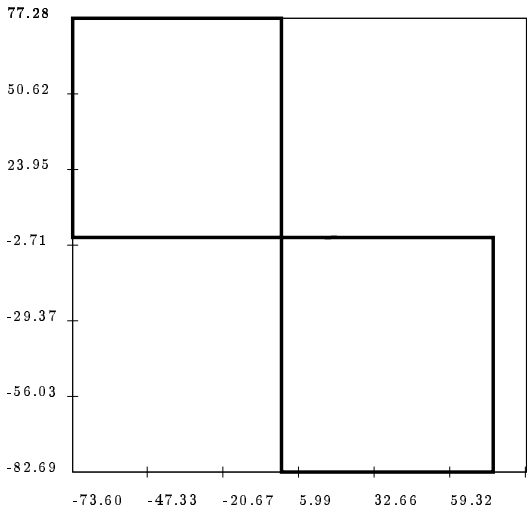

Figure 19: The region in the R_1, r_1 plane for which link 0 will interfere with some other link (trajectory 2, first set of length limit).

effectively for a robot defined by a point in the forbidden region link 0 interfere with some other link.

3.3.3 Line case

In that case the intersection of the lines occur when R_1, r_1 lie on a line D. We proceed as for the full plane case and compute the region for which the

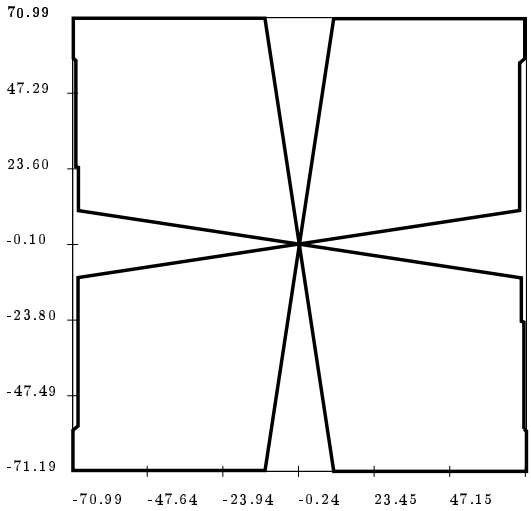

Figure 20: The region in the R_1, r_1 plane for which a pair of link will interfere (trajectory 7 (vertical motion), first set of length limit).

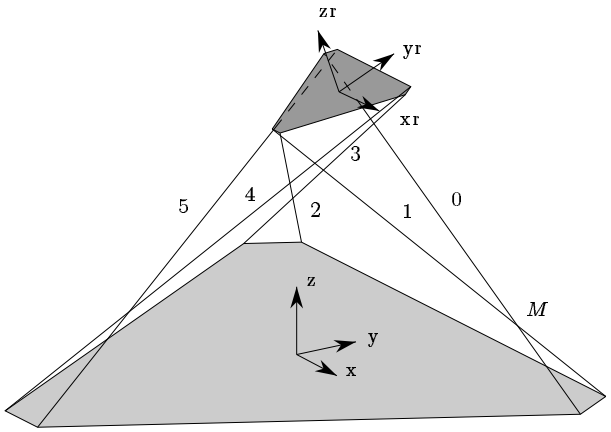

Figure 21: For a robot defined by a point in the forbidden region link 0 interfere with link 1 at point M.

inequalities are verified. Then the intersection of the resulting zones with the line D defines the segments where links interference will occur.

3.4 Verifying all the constraints

Computing the boundary of the regions which define the robots whose workspace contains the set of segments is now an easy task. Basically the process consist in computing the allowable and forbidden regions for each constraint, then to combine the result. Figure 22 shows an example of such zone. The

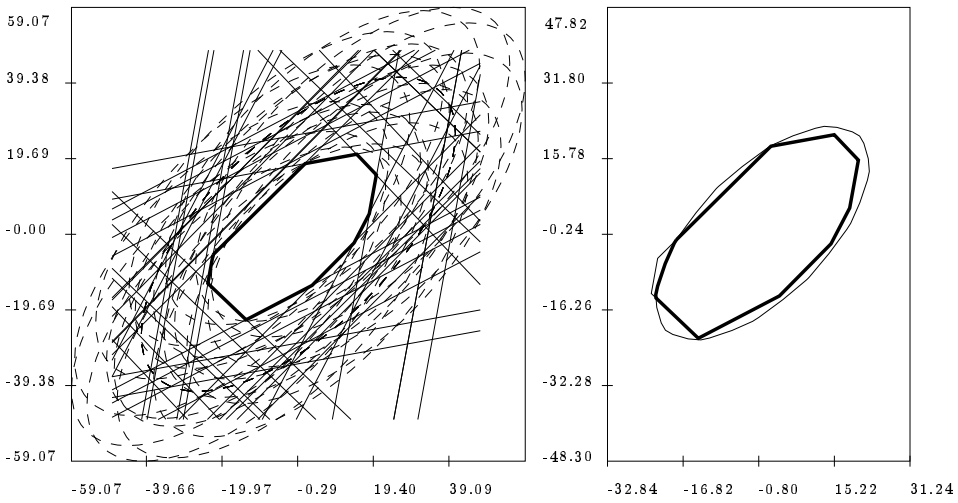

Figure 22: On the right an allowable zone for a set of constraints. Here we have computed the allowable zones for the leg lengths and the pyramids (in thin lines), then we have computed the intersection of the zones to get the final allowable zone. On the left the elements which appear during the computation of the allowable zone (trajectory 8, second set of length limits).

same input data has been used for figure 23 but interference between links have also been considered. This figure shows that effectively the two trajectories lie inside the workspace of a robot whose parameters have been taken inside the allowable region.

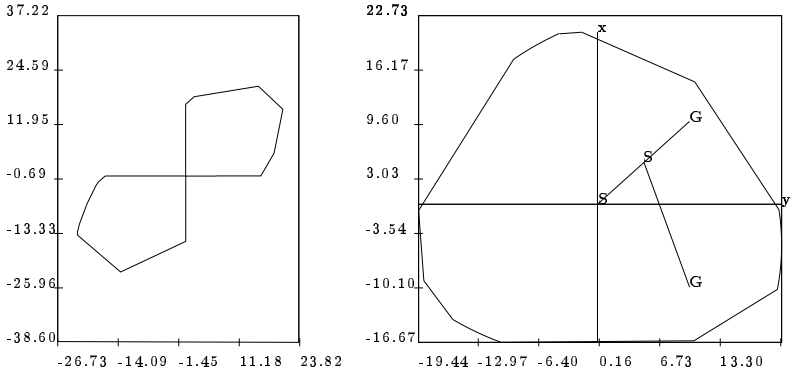

Figure 23: An allowable zone for the whole set of constraints. This is the same example as in the previous figure but links interference have been taken into account. A robot has been defined by taking the values of R_1, r_1 inside the allowable region. The figure presents the workspace boundary and the trajectories.

3.5 Changing the fixed parameters

In some case an empty zone may result from the previous computations. Therefore the fixed parameters (either the α, β angles or the leg length limits) should be modified. But we we would like to know what are the limit values for getting a non empty result. This can be done in some cases.

3.5.1 Changing the maximal length limit

A cause of failure can be that the maximal ellipse does not exist for the extreme points of the trajectory. The equation of the maximal ellipse can be written as:

$$R_1^2 + r_1^2 + C_1 R_1 r_1 + D_1 R_1 + E_1 r_1 + F_1 - \rho_{max}^2 = 0 \qquad (29)$$

where $C_1 \leq 2$. This equation is a second order equation in R_1 whose discriminant is:

$$\Delta = (C_1 r_1 + D_1)^2 - 4(r_1^2 + E_1 r_1 + F_1 - \rho_{max}^2)$$

which should be positive if the ellipse exists. This discriminant is a second order equation in r_1 whose leading term coefficient is negative. Consequently Δ will be positive only if it has two real roots or equivalently if its discriminant Δ_1 is positive:

$$\Delta_1 = -C_1 D_1 E_1 + E_1^2 + C_1^2 F_1 + D_1^2 - 4F_1 + \rho_{max}^2(4 - C_1^2)$$

which is positive if:

$$\rho_{max}^2 > \frac{C_1 D_1 E_1 - E_1^2 - C_1^2 F_1 - D_1^2 + 4F_1}{-C_1^2 + 4}$$

Consequently we can compute the minimal value of the maximal length limit so that the maximal ellipse will exist. Another case of failure will be that the maximal ellipses for the extreme points of the trajectory have no intersection. According to equation (22) these ellipses can be written as:

$$R_1^2 + r_1^2 + C_1 R_1 r_1 + (d_1 + d_0)R_1 + (e_1 + e_0)r_1 + f_2 + f_1 + f_0 - \rho_{max}^2 = 0 \quad (30)$$

$$R_1^2 + r_1^2 + C_1 R_1 r_1 + d_0 R_1 + e_0 r_1 + f_0 - \rho_{max}^2 = 0 \quad (31)$$

The resultant of these two equations is a second order equation in r_1:

$$(d_1^2 - e_1 d_1 C_1 + e_1^2)r_1^2 + (d_1^2 e_0 - e_1 d_1 d_0 + 2e_1 f_2 + 2e_1 f_1 - f_2 d_1 C_1 - f_1 d_1 C_1)r_1$$
$$+ d_1^2 f_0 - d_1^2 \rho_{max}^2 - f_2 d_1 d_0 + f_2^2 + 2f_2 f_1 - f_1 d_1 d_0 + f_1^2 = 0$$

whose discriminant Δ should be positive. The coefficient of ρ_{max}^2 in this discriminant is strictly positive and consequently a minimal value of the maximal length limit can be computed.

3.5.2 Changing the minimal length limit

A cause of failure due to the minimal length limit is that the intersection of the extremal maximal ellipses is completely inside the union of the minimal ellipses. A first possible way to solve this problem is to choose the minimum length limit so that no minimal ellipse exists. Remember that the equation of the set of minimal ellipses is

$$R_1^2 + r_1^2 + C_1 R_1 r_1 + (d_1\lambda + d_0)R_1 + (e_1\lambda + e_0)r_1 + f_2\lambda^2 + f_1\lambda + f_0 - \rho_{min}^2 = 0 \quad (32)$$

Equation (32) may be considered as a second order equation in R_1^2. Its discriminant Δ should be negative if the ellipse does not exist. Δ is a second order equation in r_1, whose leading term coefficient is strictly negative. Consequently its determinant Δ_1 must be negative. Δ_1 is a second order equation in λ with a negative leading term coefficient and therefore Δ_1 will be always negative if its discriminant Δ_2 is negative. This leads to the condition:

$$\begin{aligned}\rho_{min}^2 \quad < \quad & (4C_1^2 f_2 f_0 - C_1^2 f_1^2 - 4C_1 d_1 e_1 f_0 + 2C_1 d_0 e_1 f_1 - 4f_2 C_1 d_0 e_0 + 2C_1 d_1 e_0 f_1 - d_1^2 e_0^2 + 4 \\ & e_1^2 f_0 - e_1^2 d_0^2 + 4f_1^2 - 16 f_2 f_0 + 4 f_2 d_0^2 + 4 f_2 e_0^2 - 4 d_1 d_0 f_1 + 2 e_1 e_0 d_1 d_0 + 4 d_1^2 f_0 - 4 e_1 e_0 f_1)/ \\ & (4C_1^2 f_2 - 4C_1 d_1 e_1 + 4 d_1^2 - 16 f_2 + 4 e_1^2)\end{aligned}$$

However in some cases this inequality may lead to a negative bound for ρ_{min}^2. If this occurs we come back to the definition of the minimal and maximal ellipses. We are looking for a non empty set of R_1, r_1 such that:

$$R_1^2 + r_1^2 + C_1 R_1 r_1 + (d_1\lambda + d_0)R_1 + (e_1\lambda + e_0)r_1 + f_2\lambda^2 + f_1\lambda + f_0 - \rho_{max}^2 \leq 0 \qquad (33)$$

$$R_1^2 + r_1^2 + C_1 R_1 r_1 + (d_1\lambda + d_0)R_1 + (e_1\lambda + e_0)r_1 + f_2\lambda^2 + f_1\lambda + f_0 - \rho_{min}^2 \geq 0 \qquad (34)$$

for any $\lambda \in [0, 1]$. These equations are second order equations in λ with a positive leading term coefficient. If λ_1, λ_2 denote the roots of the first equation and λ_1', λ_2' the roots of the second one, the equations will be negative between their corresponding roots. Consequently the minimal ellipse will not exist if:

$$\lambda_2' < 0 \qquad (35)$$

$$\lambda_1' > 1 \qquad (36)$$

Condition (35) can be written as:

$$-b + \sqrt{b^2 - 4ac} < 0$$

with

$$\begin{aligned} a &= f_2 > 0 \\ b &= R_1 d_1 + R_1 e_1 + f_1 \\ c &= R_1^2 + R_1^2 + C_1 R_1 R_1 + R_1 d_0 + R_1 e_0 + f_0 - \rho_{min}^2 \end{aligned}$$

which is obtained for $b > 0, c > 0$. The first constraint defines a half-plane. The second constraints defines a forbidden ellipse. A way to maximize the possible

set of solution is to determine a value of ρ_{min} such that the forbidden ellipse does not exist. This is obtained when:

$$\rho_{min}^2 < \frac{-C_1 d_0 e_0 + e_0^2 + C_1^2 f_0 + d_0^2 - 4f_0}{(C_1 - 2)(C_1 + 2)}$$

Condition (36) can be written as:

$$\frac{-b + \sqrt{b^2 - 4ac}}{2a} > 1$$

which is obtained for $b < 0, b + a > -c$. The first constraint defines a half-plane (the complementary half-plane to the preceding case). The second constraints defines a forbidden ellipse. A way to maximize the possible set of solution is to determine a value of ρ_{min} such that the forbidden ellipse does not exist. This is obtained for:

$$\begin{aligned}\rho_{min}^2 \quad < \quad & -d_1 C_1 e_1 - d_1 C_1 e_0 - C_1 d_0 e_1 - C_1 d_0 e_0 + e_1^2 + 2e_1 e_0 + e_0^2 + C_1^2 f_1 \\ & + C_1^2 f_0 + C_1^2 f_2 + d_1^2 + 2d_1 d_0 + d_0^2 - 4f_1 - 4f_0 - 4f_2 / (C_1 - 2)(C_1 + 2)\end{aligned}$$

3.5.3 Changing the passive joints

Assume that an allowable region for the length limits has been determined. According to some criteria a point X (i.e. a robot) has been chosen in the region. It may happen that when adding the constraint on the passive joints this point is no more inside the allowable region for this constraint. This means that at least one of the faces of the constraint pyramids is such that during the trajectory the link belongs to the exterior of the pyramid as defined by the face. This face is defined by its external normal $\mathbf{n}$ which can be written as:

$$\mathbf{n} = \begin{pmatrix} \sin\mu \sin\gamma \\ -\sin\mu \cos\gamma \\ \cos\mu \end{pmatrix}$$

where μ is the angle defining the "opening" of the pyramid. According to the definition of $\mathbf{n}$ and by choosing carefully γ, μ is in the range $[\pi/2, \pi]$. We will assume now that we want to determined the minimal value μ_{min} of μ such that X is now inside the allowable region for the passive joints constraints. The following assumptions will be made:

- γ is constant, $R_1 > 0, r_1 > 0,\ z_1 > 0, z_2 > 0$

If the constraint is satisfied then:

$$\mathbf{AB}.\mathbf{n} \leq 0 \quad \forall\ \lambda\ \in\ [0,1] \tag{37}$$

This equation can be written as:

$$A_1 \cos\mu + A_2 \sin\mu + A_3 \leq 0$$

We define T as $\tan(\mu/2)$ and the constraint on μ imply that T should be in the range $[1, +\infty]$. Using the classical substitution the previous inequality can be written as:

$$AT^2 + BT - A = U \leq 0$$

with

$$A = \lambda(z_1 - z_2) - z1 - r_1 \sin(\theta)\sin(\phi + \beta) = a_1 - r_1 a_2$$

and B defines a pencil of lines in the R_1, r_1 plane. The associated equation is:

$$AT^2 + BT - A = 0 \tag{38}$$

which has always two real roots. Note also that $a_1 < 0$. Assume that $a_2 < 0$, which means that for any values of r_1 such that

$$r_1 > \frac{a_1}{a_2}$$

A is positive. In that case U will be negative when T has a value between the two real roots of equation (38). The value of the greater root T_2 is:

$$T_2 = \frac{-B + \sqrt{B^2 + 4A^2}}{2A}$$

If $B > 0$ as $\sqrt{B^2 + 4A^2} \leq B + 2A$ we deduce that $T_2 \leq 1$. Consequently there is no solution in the range $[1, +\infty]$ to our problem. As this case is not possible we deduce that this configuration cannot occur. If $B < 0$ let denote T_i:

$$T_i = \mathrm{Max}_{\lambda\ \in\ [0,1]} T_2$$

For any value of $T > \text{Max}(T_i, 1)$ the constraint on the passive joint for the particular face will be satisfied. Finding T_i is not a trivial task but we can determine a lower bound of its value. First we note that

$$T_2 \leq \frac{-B + A}{A} = T_2^1$$

The lower bound of T_i is therefore:

$$T_i = \text{Max}_{\lambda \in [0,1]} T_2^1$$

The derivative of T_2^1 with respect to λ happen to be constant. Consequently T_i is bounded by the maximum value of T_2^1 obtained either for $\lambda = 1$ or $\lambda = 0$. Note that this result is valid only if:

- $a_2 < 0$
- $r_1 > \frac{a_1}{a_2}$,
- R_1 lie in the half-plane defined by B such that B is always negative for any value of λ in [0,1].

We have now to consider the case where $A < 0$ which is obtained in two cases:

$$a_2 < 0 \qquad r_1 < \frac{a_1}{a_2}$$
$$a_2 > 0$$

In that case the inequality (37) is satisfied if T lie outside the interval of the roots. In that case the greater root T_2 is:

$$T_2 = \frac{-B - \sqrt{B^2 + 4A^2}}{2A}$$

and denote T_i:

$$T_i = \text{Max}_{\lambda \in [0,1]} T_2$$

For any value of $T > \text{Max}(T_i, 1)$ the constraint on the passive joint for the particular face will be satisfied. If $B < 0$, T_2 is lower than 1 and consequently any T is solution to the problem. If $B > 0$ a lower bound of T_2 is $1 - B/A$ which has a constant derivative with respect to λ. Consequently for any T greater than $\text{Max}(1 - B/A)_{\lambda=0,1}$ the constraint on the passive joint will be satisfied.

4 Spheres workspace

We will assume now that the desired workspace is described by a set of spheres $\mathcal{S}_i$ of radius r_i centered at M_i^1.

4.1 Forbidden region for the minimum length constraint

The following theorem hold:

Theorem 8 *For a given sphere in the desired workspace the forbidden region is an ellipse*

Proof: The demonstration uses the "growing" algorithm which enable to compute the forbidden region. The grown volume of the sphere of radius r_i centered at M_i^1 is clearly a sphere centered at M_i^1 of radius $r_i + \rho_{min}$. The intersection of the plane Π with this sphere is a circle which leads to an ellipse in the $O, \mathbf{u}, \mathbf{v}$ frame.

4.2 Allowable region for the maximum length constraint

4.2.1 The "shrinking" algorithm

To compute the allowable region we will use an algorithm similar to the "growing" algorithm. Let M be a point on the Π plane such that $\mathbf{MO} = R_1\mathbf{u} + r_1\mathbf{v}$. The allowable region is defined as the set of points M (which defines a unique value of R_1, r_1) such that:

$$||\mathbf{AB}||^2 = ||\mathbf{MC}||^2 \leq \rho_{max}^2 \tag{39}$$

for *each* point in the sphere. We have therefore to determine the volume, which will be called the "shrank" volume, such that each point inside the volume is at a distance less than or equal to ρ_{max} from the sphere. Clearly the shrank volume of a sphere of radius r centered at M is a sphere centered at M of radius $\rho_{max} - r$. Consequently the following algorithm hold:

Theorem 9 *For a given sphere in the desired workspace the allowable region is an ellipse.*

Proof: The allowable region is the intersection of the shrank volume with the plane Π and consequently a circle. In the $O, \mathbf{u}, \mathbf{v}$ frame this circle is transformed into an ellipse.

4.3 Allowable region for the mechanical limits on the joints

We may define any point P of the desired workspace by:

$$\mathbf{OP} = \mathbf{OM_i} + r\mathbf{w} \tag{40}$$

where $\mathbf{w}$ represents any vector whose norm is at most 1. The allowable region is defined by:

$$\mathbf{A_iB_i}.\mathbf{n_j^i}^T \leq 0 \quad \forall\ j\ \in\ [1,k]$$

For a given $\mathbf{n_j^i}$ this equation can be rewritten as:

$$(R_1\mathbf{u} + r_1\mathbf{v} + \mathbf{OM_i} + r\mathbf{w}).\mathbf{n_j^i}^T \leq 0 \tag{41}$$

Clearly the left side of this inequality is maximum when $\mathbf{w} = \mathbf{n_j^i}$. Consequently the half plane whose boundary is defined by the line

$$R_1\mathbf{u}.\mathbf{n_j^i}^T + r_1\mathbf{v}.\mathbf{n_j^i}^T + \mathbf{OM_i}.\mathbf{n_j^i}^T + r = 0$$

is the allowable region for the particular face of the pyramid we have considered. The half planes are computed for each face and their intersection defines the allowable region for the mechanical limits on the joint.

4.4 Forbidden region for interference between links

We will consider the case where $i = 1$ and $j = 2$ without loss of generality. If the two lines intersect then:

$$\mathbf{A_1A_2}.(\mathbf{A_1B_1} \times \mathbf{A_2B_2})^T = 0 \tag{42}$$

which can be written as:

$$-R_1r_1(b_1R_1 + b_2r_1 + b_3 + \mathbf{u'}.\mathbf{w}^T) = 0 \tag{43}$$

where $\mathbf{u}'$ is a constant vector. We will assume without loss of generality that $R_1 > 0, r_1 > 0$. Let us consider the region $\mathcal{R}$ bounded by the two lines:

$$b_1 R_1 + b_2 r_1 + b_3 \pm ||\mathbf{u}'|| = 0$$

In this region it always exists a vector $\mathbf{w}$ such that equation (43) is satisfied. Now we consider the inequalities (8, 9),(10,11) which have all the same generic form:

$$e_1 R_1 + e_2 r_1 + e_3 + \mathbf{v}'.\mathbf{w}^T \leq 0$$

where $\mathbf{v}'$ is a constant vector. Consider the two half planes separated by the line

$$e_1 R_1 + e_2 r_1 + e_3 + ||\mathbf{v}'|| = 0$$

One of this half plane is such that for every R_1, r_1 it exists $\mathbf{w}$ such that the inequality is satisfied. The four inequalities define four half planes whose intersection with $\mathcal{R}$ defines the forbidden region for the interference between the links.

5 Extension to other types of desired workspace

As the number of objects used to specify the desired workspace is not limited we may assume that any volume may be approximated by a finite set of segments, points and spheres. However it would be interesting to consider other types of geometric objects to define the desired workspace. Note that for the length constraints we may use the "growing" and "shrinking" algorithm for any type of object, although the computation of the intersection between the grown volume, the shrank volume and the plane Π may be difficult. We will consider here the case where polygons or polyhedron are used to describe the desired workspace.

5.1 Allowable regions for the length constraints

The following theorem hold:

Theorem 10 *The allowable region for the maximum links length constraint is the intersection of the maximal ellipses computed for the vertices of the polygons (polyhedron)*

Proof: Let $\mathcal{I}$ be the intersection of the maximal ellipses computed for the vertices of the polygon and $\mathcal{A}$ the allowable region. Clearly $\mathcal{A} \subset \mathcal{I}$. Using the result of the segments workspace section any point in $\mathcal{I}$ defines an allowable robot with respect to the maximal length constraints for any point on the edge of the polygon. This result hold for any point on a segment joining two points on two arbitrary edges of the polygon. As any point inside the polygon is on such segment $\mathcal{I} \subset \mathcal{A}$, which complete the proof.
The following theorem is a corollary:

Theorem 11 *The allowable region for a concave polygon (polyhedra) is identical to the allowable region of its convex hull.*

Proof: Note that the workspace of the robot with respect to the maximum length constraint is the intersection of the spheres of radius ρ_{max_i} centered at $\mathbf{OA_i} + \mathbf{B_iC}$. Consequently this workspace is convex and the convex hull of any polygon belonging to the workspace will also belong to the workspace.

Unfortunately the previous results does not hold for the minimum links length constraint. Consequently the "growing" algorithm has to be used, this task being not very difficult.

5.2 Allowable regions for the passive joint constraints

We assume here that the workspace is defined by one polygon. For every vertex V of this polygon we consider the half-plane in the R_1, r_1 plane defined by:

$$R_1\mathbf{u}.\mathbf{n}^T + r_1 R\mathbf{v}.\mathbf{n}^T + \mathbf{OV}.\mathbf{n}^T \leq 0 \tag{44}$$

We note that the support line of this half-plane has the same slope whatever is the vertex V. We remark also that the half-plane lie on the same side of the support line whatever is V. Let H_i be the set of half-planes. We define the *minimal half-plane*H_{min} *associated to the normal* $\mathbf{n}$ *and the set* H_i as the intersection of the H_i. The following theorem is trivial:

Theorem 12 *Let H_i be a set of two half-planes associated to two vertices V_1, V_2 of the workspace polygon and H_{min} the minimal half-plane associated to this set and to a normal of a pyramid face. Then H_{min} defines the allowable region for the trajectory segment V_1V_2 with respect to the face.*

Now we can establish the main theorem:

Theorem 13 *Let H_i be a set of half-planes associated to all the vertices of the workspace polygon and H_{min} the minimal half-plane associated to this set and to a normal of a pyramid face. Then H_{min} defines the allowable region for the workspace polygon with respect to the face.*

Proof: Let H_s be the allowable region for the workspace polygon. Clearly

$$H_s \subset H_{min}$$

Consider the segment joining two vertices of the workspace polygon and H_t the allowable region for this segment. According to the previous theorem:

$$H_{min} \subset H_t$$

Now consider any segment between two points X_1, X_2 on the hull of the workspace polygon and the minimal half-plane H_{12} associated to this point. Let V_1, V_2 be the vertices between which lie X_1 and V_3, V_4 the vertices between which lie X_2 and H_{14} the minimal half-plane for this set of vertices. Clearly

$$H_{14} \subset H_{12}$$

As $H_{min} \subset H_{14}$ we have $H_{min} \subset H_{12}$. For any point X between X_1, X_2 the corresponding region include H_{12} and consequently H_{min}. As any point in the polygon is on such segment we deduce that H_{min} is a subset of H_s and consequently $H_s = H_{min}$.
The following theorem is a corollary

Theorem 14 *The allowable region for a workspace polygon is identical to the allowable region of the convex hull of the workspace polygon.*

Computing the allowable region for a complete pyramid can be done simply by first computing the minimal half-planes for the set of vertices of the workspace polygon for all the faces and then taking the intersection of these half-planes.

5.3 Allowable region for links interference

In this section we will assume that the links have no thickness. We want to determine the zone in the R_1, r_1 plane for which there is no interference between any pair of links, i.e. the zone for which the intersection point M between the line going through A_i, B_i and A_j, B_j, if any, does not belong to both A_iB_i, A_jB_j. We will consider the case where $i = 1$ and $j = 2$ without loss of generality.

5.3.1 Basic equations

If the two lines intersect for some location of the mobile platform then:

$$\mathbf{A_1A_2}.(\mathbf{A_1B_1} \times \mathbf{A_2B_2})^T = 0 \tag{45}$$

which can be written as:

$$-R_1r_1(b_1R_1 + b_2r_1 + b_3) = 0 \tag{46}$$

where b_1, b_2 are independent of the location of the platform and

$$b_3 = b_{31}x + b_{32}y + b_{33}z$$

where x, y, z are the coordinates of a point inside the polygon. Various cases can now be considered:

1. if the coefficients b_i are general the lines will intersect if the R_1, r_1 are on a line in the R_1, r_1 plane
2. if $b_1 = b_2 = b_3 = 0$ the lines intersect whatever are the dimensions of the robot.
3. if $b_1 = b_2 = 0, b_3 \neq 0$ the lines never intersect whatever are the dimensions of the robot.

Now consider every location of the platform which lie inside the workspace polygon. If $b_1 \neq 0$ or $b_2 \neq 0$ the location of the R_1, r_1 such that the lines intersect is a region $\mathcal{R}$ bounded by two lines described by equation (46) with same slope, whose b_3 terms are obtained for one the vertices of the convex hull of the workspace polygon.

Assume now that $b_1 = b_2 = 0$. The lines will intersect only if $b_3 = 0$ for some points of the workspace polygon. This equation defines a plane in the 3D space and three cases may occur:

- the plane has no intersection with the workspace polygon: the lines (and therefore the links) will never intersect. $\mathcal{R}$ is empty.
- the workspace polygon belongs to the plane: the lines will always intersect whatever are the dimensions of the robot. $\mathcal{R}$ is the full R_1, r_1 plane.
- the plane has an intersection line with the workspace polygon: the lines will intersect when R_1, r_1 lie on a line which is the $\mathcal{R}$ region.

Assume now that $\mathcal{R}$ is not an empty region. In the same manner as for the points workspace we want to investigate if there is a subset of $\mathcal{R}$ for which the links will interfere defined by the inequalities (8,9), (10,11) . The quantities which appear on the left side of the inequalities can be expressed as functions of R_1, r_1. They have all the same generic form:

$$R_1(e_1R_1 + e_2r_1 + e_3) \quad \text{or} \quad r_1(e_1R_1 + e_2r_1 + e_3)$$

where the e_1, e_2 coefficients does not depend upon the location of the platform.

5.3.2 Computing the allowable region

One way to deal with the inequalities problem is to use the four-dimensional space R_1, r_1, x, y. In this space each inequality defines an half space whose boundary is an hyper plane. The intersection of the four half spaces defines a region $\mathcal{S}$. Note that this region is a four dimensional pyramid as its boundary is the intersection of the half spaces who have the origin in common. But we are interested in the sub-region of $\mathcal{S}$ such that x, y belongs to the workspace polygon. So we project the workspace polygon on the x, y plane and consider the hyper volume delimited by this projection. The intersection of this hyper volume with $\mathcal{S}$ defines the region in which interference between links will occur. The boundary of the projection of this region on the R_1, r_1 plane is the boundary of the allowable region with respect to the inequalities. Figure 24 is a tentative explanation of this process when used in a 3D space. As soon as this region is computed its intersection with $\mathcal{R}$ defines the allowable region.

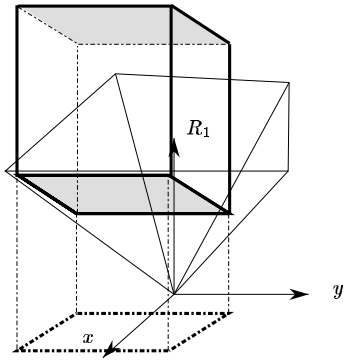

Figure 24: Tentative explanation of the computation of the allowable region adapted to a 3D case. The four inequalities define a pyramidal region whose apex is the origin. For any point inside the region the inequalities are satisfied. We consider the sub-region of the pyramid (in thick line) such that its projection on the x, y plane is identical to the projection of the workspace polygon (in thick dashed line). By projecting this sub-region on the R_1, r_1 plane we get the allowable region with respect to the inequalities.

6 Extension to other types of parallel manipulators

The algorithm described in this paper was illustrated on the Gough-type parallel manipulator. But a similar algorithm can be used for other types of parallel robots.

6.1 INRIA active wrist

For example consider the 6 D.O.F. robot, called the *active wrist*, described by Merlet [13] (figure 25), which has been used for eye surgery [7]. For this type of

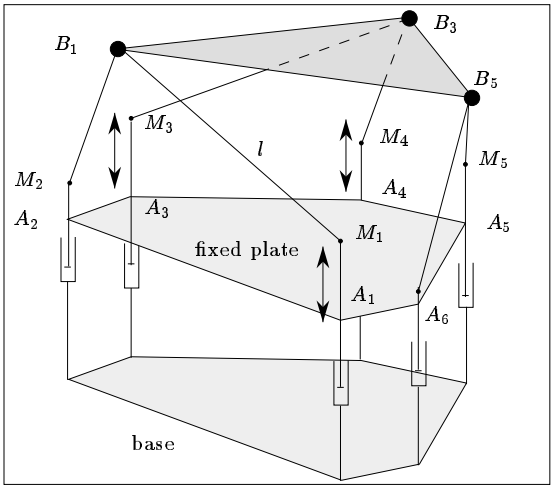

Figure 25: The INRIA robot

robot a linear actuator enables to move the extremity M_i of the link A_iM_i along a vertical axis (A_i is the center of the hole on the fixed plate through which slide the actuator). The platform is connected to this link through the link M_iB_i which has a ball-and-socket joint and an universal joint at its extremities. The posture of the moving platform can therefore be controlled by the distance ρ_i between A_i, M_i (i.e. the height of M_i with respect to the fixed plate). We will

study now the inverse kinematics of this robot. Let l_i be the fixed length of link M_iB_i. We have

$$||\mathbf{M_iB_i}||^2 = l_i^2 = ||\mathbf{M_iA_i} + \mathbf{A_iB_i}||^2 \tag{47}$$

with $\mathbf{M_iA_i} = -\rho_i \mathbf{z}$. This lead to:

$$\rho_i^2 - 2\rho_i \ \mathbf{z}.\mathbf{A_iB_i} + \mathbf{A_iB_i}^2 - l_i^2 = 0 \tag{48}$$

Note that we may get two solutions to this equation which are either lower or greater than the z coordinate of B_i. We will assume here we are interested only in the lowest value, B_i being always over M_i Let us assume now that we have defined the desired workspace as a given posture and that the value of ρ_i should be in the range $[\rho_{min}, \rho_{max}]$. Using the same development as for the Gough-type platform we get that for a fixed value of ρ equation (48) defines an ellipse in the R_1, r_1 plane. Consider now each point Q of the R_1, r_1 plane such that:

$$\rho_{max}^2 - 2\rho_{max} \ \mathbf{z}.\mathbf{A_iB_i} + \mathbf{A_iB_i}^2 - l_i^2 \leq 0 \tag{49}$$

i.e. the interior of the maximal ellipse. Assume now that for a point Q there exists a value of ρ such that equation (48) is satisfied. We subtract these two equations to get:

$$\rho_{max}^2 - 2\rho_{max} \ \mathbf{z}.\mathbf{A_iB_i} - \rho^2 + 2\rho \ \mathbf{z}.\mathbf{A_iB_i} \leq 0 \tag{50}$$

or

$$(\rho_{max} - \rho)(\rho_{max} - 2 \ \mathbf{z}.\mathbf{A_iB_i} + \rho) \leq 0 \tag{51}$$

Note that $\mathbf{z}.\mathbf{A_iB_i} > 0$. If we assume that the right term of this inequality is positive, then the value of ρ corresponds to the solution where M_i is over B_i. According to our assumption we may therefore state that this term is negative. Consequently this inequality is satisfied iff $\rho \leq \rho_{max}$ and the maximal ellipse defined the allowable region with respect to the maximum height constraint. A similar reasoning would show that the minimal ellipse is also the forbidden region with respect to the minimum height for the actuator. Therefore the algorithm developed for the Gough-type platform can be applied for this robot.

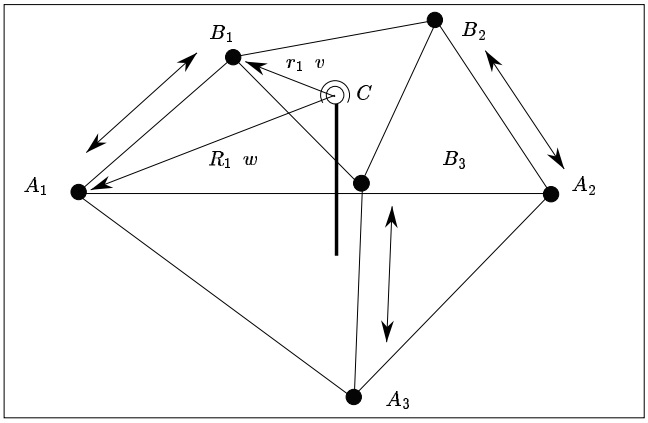

Figure 26: 3 D.O.F. wrist

6.2 Three D.O.F. wrist

The proposed algorithm works also with less than 6 D.O.F. robot. Consider for example the 3 D.O.F. rotational wrist described in figure 26. Basically this robot is similar to a Gough-type platform except that the platform is constrained by a ball-and-socket joint, enabling only rotation around C. The rotation motion is obtained by changing the length of the link A_iB_i. We assume that the attachment points A, B lie on lines going through C with unit vectors $\mathbf{w}$, $\mathbf{v}$. The design parameters are the distances R_1, r_1 between (C, A), (C, B). The length of the link for a given $\mathbf{v}$ is:

$$\rho^2 = R_1^2 + r_1^2 + 2R_1 r_1 \mathbf{w}.\mathbf{v}^T$$

The desired workspace is specified by the possible values of $\mathbf{v}$. Let v_m, v_M the minimum and maximum values of $\mathbf{w}.\mathbf{v}^T$ over the desired workspace. The allowable region for the maximum length constraint will be the ellipse defined by:

$$R_1^2 + r_1^2 + 2R_1 r_1 v_M - \rho_{max}^2 \leq 0$$

The forbidden region for the minimum length constraint will be the ellipse defined by:

$$R_1^2 + r_1^2 + 2R_1 r_1 v_M - \rho_{min}^2 \leq 0$$

7 Conclusion

The algorithm presented in this paper enables to compute all the possible locations of the attachment points of the robots whose workspace contains a desired workspace. Afterward some other criterion can be used to determine an "optimal" robot using a numerical algorithm with a search domain which is now considerably restricted. The possible criterion might be:

- the maximal dexterity over the workspace
- to minimize the maximum of the articular forces when the robot moves a given load in the specified workspace
- to minimize the maximum of the positioning errors for the platform for a given error of the sensors measuring the leg length
- to maximize the maximal velocity of the platform for given velocities of the actuators
- the robot with no singularities in the workspace

The last point can be solved by computing the singularities surfaces of the robot using the method described in [10] and checking their intersection with the specified workspace. The remaining points are still open problem and will constitute the object of our future research.

8 Annexes

8.1 Numerical data of the examples

8.1.1 Angles α_i, β_i

Angles α_i, β_i in degree

link	1	2	3	4	5	6
α_i	35	145	155	265	275	25
β_i	85	95	205	215	325	335

8.1.2 Length limits

Minimum and maximum length of the legs (first set)

30	30	30	30	30	30
40	40	40	40	40	40

Minimum and maximum length of the legs (second set)

40	40	40	40	40	40
59	59	59	59	59	59

8.1.3 Trajectories

Trajectory 0						Trajectory 2					
0	0	20	0	0	0	5	0	20	0	20	0
10	10	20	0	0	0	-10	10	20	0	20	0

Trajectory 5						Trajectory 7					
0	0	20	0	30	0	0	0	20	90	0	0
-10	10	20	0	30	0	0	0	-20	90	0	0

Trajectory 8					
0	0	50	0	0	0
10	10	50	0	0	0
5	5	50	0	0	0
10	-10	50	0	0	0

8.2 Proof of theorem 7

Under the assumption of the theorem we notice that the base and the platform are parallel. For any r_1 the point B describes a segment P_1P_2 which is parallel to M_1M_2 (figure 27). As r_1 vary the extremity of P_1P_2 moves on two lines whose angle with the x axis is equal to $\psi + \beta$ (figure 28). Now consider a special position C_s of C on M_1M_2 for a given r_1 which correspond to a special position B_s of B on P_1P_2. The corresponding A point of B_s must lie inside

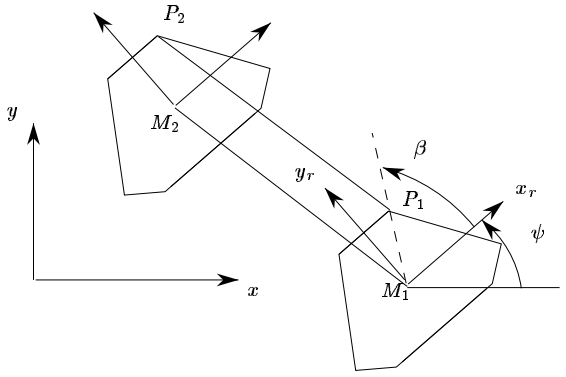

Figure 27: When C moves on a segment M_1M_2 then B moves on a segment P_1P_2 parallel to M_1M_2.

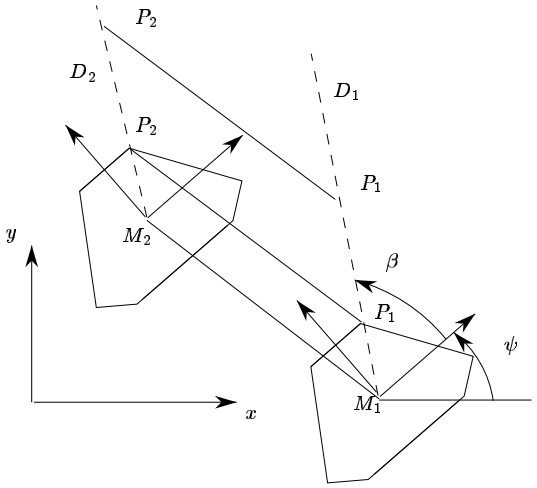

Figure 28: When r_1 vary the extremity of P_1P_2 lie on two lines D_1, D_2

the sphere of center B_s and radius ρ and simultaneously in the base plane. Consequently the A point must lie inside a circle with a defined radius r. Note that the radius of this circle is independent of C_s and r_1 as the platform and base plane are parallel. The maximum and minimum values R_1^{max}, R_1^{min} of R_1 are then obtained by taking the intersection of the circle with the line D_{R1} on which lie R_1 (figure 29). Now assume that r_1 may vary for this given C_s and

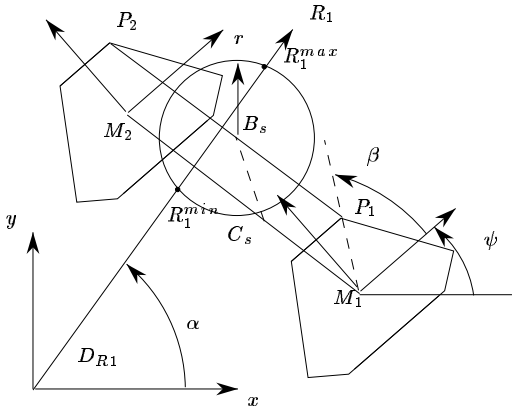

Figure 29: For a given position C_s of C and a given r_1 R_1 must be included in a circle. The intersection of this circle and the line D_{R1} on which lie R_1 define the minimum and maximum values R_1^{min}, R_1^{max} of R_1.

that we want to compute the maximum and minimum values R_1^M, R_1^m of R_1. Therefore we have to find the position of B_s on its line D_s such that R_1 is extremal. This is obtained when the circle centered on D_{R1} is exactly tangent with the line D_s (figure 30). For any position of C on M_1M_2 the center of the circle will move on a line and the angle between this line and D_{R1} is always the same. As the radius of the circle does not depend upon $r1, C$ this means that for any C the value of $R_1^M - R_1^m$ will always be the same. Let us determine now the maximum and minimum values r_1^M, r_1^m of r_1 for a given position C_s of C. For a given R_1 the extremal value of r_1 are obtained by taking the intersection points of the circle centered at B_s with radius r and the line D_{R1}. This imply that the extremal values of r_1 are obtained when the circle centered on D_s

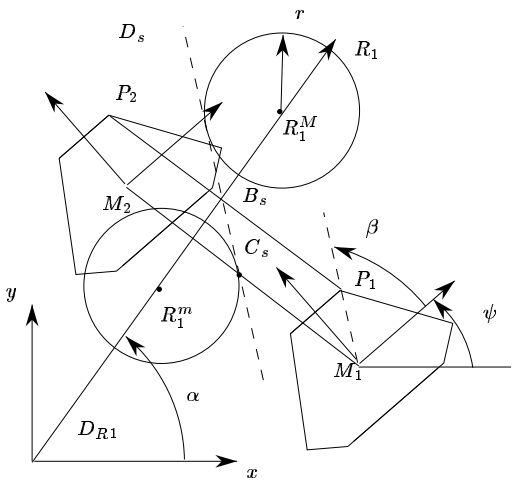

Figure 30: As r_1 vary the maximum and minimum values R_1^M, R_1^m of R_1 are obtained when the circle centered on D_{R1} is tangent to D_s.

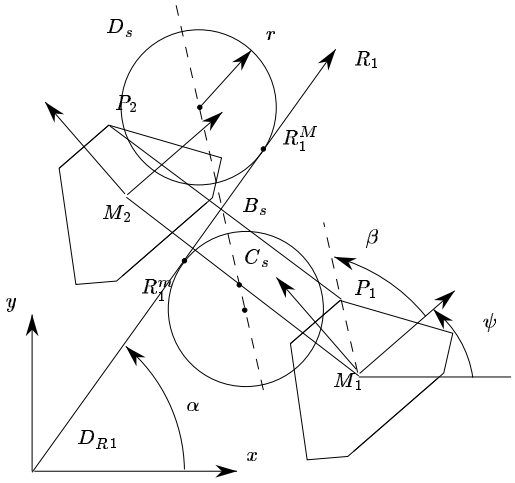

Figure 31: As R_1 vary the maximum and minimum values r_1^M, r_1^m of r_1 are obtained when the circle centered on D_s is tangent to D_{R1}.

is tangent to D_{R1} (figure 31). In the same manner as for R_1 the difference between r_1^M and r_1^m does not depend on C_s.

Consequently we have shown that for any point C on M_1M_2 the ellipse whose orientation is always the same is included in a box whose dimensions does not depend on the location of C. Therefore the dimension of the ellipse is independent of the location of C and this complete the proof of the first part of the theorem.

Note now that the proof is only dependent of the fact that the radius of the circle is constant and that the angle between D_s and D_{R1} is constant. The value of this angle is $\psi + \beta$ and therefore independent of the choice of M_1, M_2. Thus for any trajectory the dimension of the ellipse is constant.

References

[1] Claudinon B. and Lievre J. Test facility for rendez-vous and docking. In *36th Congress of the IAF*, pages 1–6, Stockholm, October 7-12, 1985.

[2] Dubowsky S. and others . The design and implementation of a laboratory test bed for space robotics: the VES mod. II. In *ASME Design Automation Conf.*, Minneapolis, September 14-16, 1994.

[3] Gosselin C. *Kinematic analysis optimization and programming of parallel robotic manipulators.* Ph.D. Thesis, McGill University, Montréal, June 15, 1988.

[4] Gosselin C. Determination of the workspace of 6-dof parallel manipulators. *J. of Mechanical Design*, 112(3):331–336, September, 1990.

[5] Gosselin C. and Angeles J. The optimum kinematic design of a planar three-degree-of-freedom parallel manipulator. *J. of Mechanisms, Transmissions and Automation in Design*, 110(1):35–41, March, 1988.

[6] Gosselin C., Lavoie E., and Toutant P. An efficient algorithm for the graphical representation of the three-dimensional workspace of parallel manipulators. In *22nd Biennial Mechanisms Conf.*, pages 323–328, Scotsdale, September 13-16, 1992.

[7] Grace K.W. and others . A six degree of freedom micromanipulator for opthalmic surgery. In *IEEE Int. Conf. on Robotics and Automation*, pages 630–635, Atlanta, May 2-6, 1993.

[8] Liu K., Fitzgerald M.K., and Lewis F. Some issues about modeling of the Stewart platform. In *2nd Int. Symp. on Implicit and Robust systems*, Warsaw, 1991.

[9] Liu K., Fitzgerald M.K., and Lewis F. Kinematic analysis of a Stewart platform manipulator. *IEEE Trans. on Industrial Electronics*, 40(2):282–293, April, 1993.

[10] Merlet J-P. Singular configurations of parallel manipulators and Grassmann geometry. *The Int. J. of Robotics Research*, 8(5):45–56, October, 1989.

[11] Merlet J-P. Détermination de l'espace de travail d'un robot parallèle pour une orientation constante. *Mechanism and Machine Theory*, 29(8):1099–1113, November, 1994.

[12] Merlet J-P. Trajectory verification in the workspace for parallel manipulators. *The Int. J. of Robotics Research*, 13(4):326–333, August, 1994.

[13] Merlet J-P. and Gosselin C. Nouvelle architecture pour un manipulateur parallèle à 6 degrés de liberté. *Mechanism and Machine Theory*, 26(1):77–90, 1991.

[14] Sternheim F. Tridimensionnal computer simulation of a parallel robot. Results for the Delta 4 machine. In *18th Int. Symp. on Industrial Robot*, pages 333–340, Lausanne, April 26-28, 1988.

[15] Stoughton R. and Kokkinis T. Some properties of a new kinematic structure for robot manipulators. In *ASME Design Automation Conf.*, pages 73–79, Boston, June 28, 1987.

[16] Troyanov M., April, 1994. Prolégomènes n° 11.

Contents

Unité de recherche INRIA Lorraine, Technopôle de Nancy-Brabois, Campus scientifique,
615 rue du Jardin Botanique, BP 101, 54600 VILLERS LÈS NANCY
Unité de recherche INRIA Rennes, Irisa, Campus universitaire de Beaulieu, 35042 RENNES Cedex
Unité de recherche INRIA Rhône-Alpes, 46 avenue Félix Viallet, 38031 GRENOBLE Cedex 1
Unité de recherche INRIA Rocquencourt, Domaine de Voluceau, Rocquencourt, BP 105, 78153 LE CHESNAY Cedex
Unité de recherche INRIA Sophia-Antipolis, 2004 route des Lucioles, BP 93, 06902 SOPHIA-ANTIPOLIS Cedex

Éditeur
INRIA, Domaine de Voluceau, Rocquencourt, BP 105, 78153 LE CHESNAY Cedex (France)
ISSN 0249-6399